8-10-2021

Double-Layered M2e-NA Nanoparticles Induce Broad Protection Against Different Influenza Viruses in Mice

Ye Wang

Double-Layered M2e-NA Nanoparticles Induce Broad Protection Against Different Influenza Viruses in Mice

by

Ye Wang

Under the Direction of Baozhong Wang, Ph.D.

A Dissertation Submitted in Partial Fulfillment of the Requirements for the Degree of

Doctor of Philosophy

in the College of Arts and Sciences

Georgia State University

2021

ABSTRACT

The development of a universal influenza vaccine is an ideal strategy to eliminate public health threats from influenza epidemics and pandemics. Influenza conserved structures are outstanding immunogens for such a vaccine. Layered protein nanoparticles composed of well-designed conserved influenza structures have improved immunogenicity with new physical and biochemical features. We constructed and purified structure-stabilized influenza matrix protein 2 ectodomain (M2e) and M2e-neuraminidase fusion proteins (M2e-NAs). We produced double-layered M2e-NA protein nanoparticles by chemical crosslinking M2e-NA onto M2e nanoparticle surfaces. Immunizations with these protein nanoparticles induced immune protection against influenza viruses with homologous and heterosubtypic NA in mice. Double-layered M2e-NA protein nanoparticles induced higher levels of humoral and cellular responses compared with their comprising protein mixture or M2e nanoparticles. In addition, the layered M2e-NA protein nanoparticle group demonstrated strong cytotoxic T cell responses. We also found that antibody responses contributed to heterosubtypic influenza viral immune protection. The protective immunity was long-lasting.

To favorite rapid distribution and convenient administration of a universal influenza vaccine, we incorporated the FliC-adjuvanted M2e-NA nanoparticles into logistically simple microneedle patches (MNPs) for skin vaccination in mice. The nanoparticle MNPs significantly increased M2e and NA-specific antibody levels, the numbers of germinal center B cells, and IL-4 secreting splenocytes. MNPs incorporating the double-layered nanoparticles protected mice against homologous and heterosubtypic influenza viruses. Our results demonstrated that M2e-NA nanoparticles could be developed into a standalone or synergistic component of a universal

influenza vaccine strategy. MNP skin vaccination can logistically simplify the vaccines for extensive distribution and administration.

INDEX WORDS: Influenza NA protein nanoparticle, M2e, Universal influenza vaccine, Flagellin, Skin vaccination, Dissolvable microneedle patch

Double-Layered M2e-NA Nanoparticles Induce Broad Protection Against Different Influenza Viruses in Mice

by

Ye Wang

Committee Chair: Baozhong Wang

Committee: Sang-Moo Kang

Timothy Denning

Electronic Version Approved:

Office of Graduate Services

College of Arts and Sciences

Georgia State University

August 2021

DEDICATION

The thesis is dedicated to my parents for their affection, love, and generous spirit and material support to me.

ACKNOWLEDGEMENTS

The completion of this study would not have been possible without the expertise of my advisor, Dr. Baozhong Wang. During the past four years, he devoted much time to my research project, including the project direction, manuscript publication, even the operation of specific experiments. I would also like to thank Dr. Sang-Moo Kang and Dr. Timothy Denning for reviewing my dissertation.

A debt of gratitude is also owed to Dr. Lei Deng, Dr. Chunhong Dong, Dr. Yao Ma, Gilbert Gonzalez, and Dr. Wandi Zhu for providing me with the guides for experiments.

Last but not least, I would like to thank my parents, Mr. Kai Wang, and Mrs. Qin Zhao. Without you, none of this would indeed be possible.

TABLE OF CONTENTS

LIST OF FIGURES

LIST OF ABBREVIATIONS

Abbreviations	Full names
ADCC	Antibody dependent cellular cytotoxicity
ADCP	Antibody dependent cellular phagocytosis
AF488	Alexa Fluor 488
BMDC	Bone marrow dendritic cells
CTL	Cytotoxic lymphocyte
DC	Dendritic cells
DTSSP	3,3'-Dithiobis(sulfosuccinimidylpropionate)
E.coli	Escherichia coli
FliC	Flagellin
GC	Germinal center
IFN	Interferon
IL	Interleukin
ILN	Inguinal lymph nodes
IM	Intramuscular(ly)
IN	Intranasal(ly)
IP	Intraperitoneal
LD50	Median Lethal Dose
M2e	Matrix protein 2 ectodomain
M2e-N1 nano	M2e-N1 nanoparticle
M2e-N2 nano	M2e-N2 nanoparticle
MDCK	Madin-Darby Canine Kidney
MFN	NA-FliC/M2e nanoparticle
MN	NA/M2e nanoparticle
MNP	Microneedle patch
NA	Neuraminidase
rViet	Recombinant Vietnam (H5N1) influenza virus
sM2e+N1	Soluble M2e + soluble Neuraminidase 1
sM2e+N2	Soluble M2e + soluble Neuraminidase 2
sMFN	Soluble M2e + NA + FliC
TCID50	Median Tissue Culture Infectious Dose
TLR	Toll-like receptor

INTRODUCTION

Influenza continuously poses a severe public health risk and causes pandemics. Another severe influenza pandemic is inevitable and just a matter of time [1, 2]. Current seasonal influenza vaccines can effectively protect healthy adults against well-matched strains, but mismatches frequently occur because of the high rate of antigenic variation in influenza surface antigens [3]. For instance, during the 2014-2015 influenza season, the overall vaccine effectiveness was very low, estimating an adjusted 19% in the US because the major circulating H3N2 viruses drifted from the vaccine strain [4]. The 2017-2018 flu season is another case of a severe outbreak of an influenza epidemic since 2009 due to a weak vaccine efficacy versus the prevalent H3N2 strain [5, 6]. Beyond epidemics, a non-human influenza virus could acquire mutations gaining the capacity for effective transmission in humans and result in an influenza pandemic [7, 8]. The outcome of such a pandemic would be catastrophic because humans have no historical immunity to such viruses.

A universal influenza vaccine will negate the need for yearly influenza vaccinations and serve as a countermeasure against the emergence of novel pandemic strains by offering universal protection. Multiple approaches have been investigated - the promising ones utilize epitopes that are conserved across different influenza virus strains as the vaccine immunogens [9-11]. However, conserved antigens (such as the ectodomain of influenza M2 protein or HA stalk domains) generally induce weak immune responses and require adjuvants to boost their potency. Delivery of protein antigens is also a challenge because of their fast degradation and diffusion upon introduction to the body.

Our laboratory has studied solid protein nanoparticles (nanoclusters) as a universal influenza vaccine delivery system in recent years. In this study, the protein nanoparticles comprised of

almost conserved antigenic proteins like Neuraminidase (NA), Matrix ectodomain (M2e), and a minimal amount of a reducible crosslinker. Moreover, to further simplify the vaccine for extensive distribution and convenient administration, we incorporated the flagellin (FliC)-adjuvanted nanoparticles into microneedle patches (MNPs) for painless skin vaccination.

1.1 Conserved influenza epitopes for universal influenza vaccines

The influenza virion has two highly glycosylated proteins, HA and NA, and a third ionic channel protein, M2 on its surface. Influenza virus infection can cause severe respiratory disease during the yearly influenza seasons by evading prevailing immunity via frequent mutations on the globular head of the hemagglutinin protein (HA). In recent years, the researchers focused more on the conserved structures from NA or M2 in developing a universal influenza vaccine [12].

1.1.1 The glycoprotein neuraminidase in influenza virus

Influenza neuraminidase (NA) is an important membrane glycoprotein containing four identical polypeptides. Although NA facilitate the influenza viral replication during the virus entry, receptor binding, and virus internalization, the most characterized function of NA is its catalytic activity of cleaving sialic acid and HA. Inside the catalytic site of NA, the inner eight highly conserved residues directly interact with sialic acid, while ten outer conserved residues do not contact sialic acid but provide space for the substrates [13]. Among the eight highly conserved residues, the Tyr406 is crucial for the catalytic function as a nucleophile [14]. The conserved feature of catalytic site makes NA an ideal target for anti-viral drug development.

For a long time, NA was underestimated by the vaccinology community due to its relatively poor immunogenicity and the immunodominance of HA[15]. However, recent studies have shown NA to be a promising antigen for vaccine development: (1) Compared with HA, NA experiences relatively slower antigenic drift [16]. (2) A universally conserved NA epitope between 222-230

induced NA-inhibiting antibodies against all influenza types[17, 18]. (3) Therapeutic NA-specific monoclonal antibodies protected mice from lethal doses of homologous and heterologous influenza infection[19]. Most NA antibodies do not directly neutralize the influenza virion but inhibit enzymatic activity [20]. Moreover, the non-neutralizing NA-antibody inhibit the influenza virus by FcRs mediated antibody-dependent cellular cytotoxicity (ADCC) [21]. For example, a 2009 pandemic H1N1 strain derived NA-reactive antibody, 3C05, required FcγRs during protection [22]; the H3N2 derived mAbs 1G04 can protect mice against various type of influenza virus including influenza B/Malaysia/2004 and avian virus H4N6 [23]. These discoveries demonstrated that NA has the potential to be developed into a universal influenza vaccine if it is presented in an immunogenic form, such as protein nanoparticles.

1.1.2 The ectodomain of the M2 protein (M2e)

Although much less abundant than HA, M2 is an essential protein that functions in viral assembly and morphogenesis. Upon the binding of HA to sialic acid of host cells, receptor-mediated endocytosis occurs and the whole endosome is acidified with a downregulated pH to 5 to 6. The acidic environment enable the M2 proton channel open and result in the proton influx to the virion. Then the viral ribonucleoprotein (RNP) complexes are released into the cytoplasma for the entry to nucleus [24]. The M2 extracellular domain (M2e) contains a highly conserved amino acid sequence, SLLTEVET, which is over 99% conserved among all subtype A influenza viruses [25, 26]. Compared with HA, the natural M2e is weakly immunogenic. To improve the weak immunogenicity, researchers usually combine this epitope with more immunogenic components like HA or increase the copy number of the highly conserved sequence in the tetrameric structure [27, 28].

Moreover, nanoparticles are another option to improve the immunogenicity of M2e because the conserved epitope can be loaded at high density and co-loaded with immune stimulators. For example, a fusion protein compromised of M2e, helix C of the hemagglutinin stalk domain (from H1N1 PR8 or H5N2 Penn), a universal T cell epitope, and flagellin was created. Under the right chemical conditions, the fusion protein self-assembled into 24-mer nanoparticles which carried the antigens above in their native conformations [29]. Antibody titers induced in chickens by the flagellin-adjuvanted H5N2 HA stalk domain nanoparticles conferred broad cross-protection. The H1N1 PR8 nanoparticles protected mice from a lethal dose challenge, while the mice in an inactivated virus vaccine-immunized group showed limited protection. The ferritin cage structure to carry three tandem repeats of M2e was adapted. This 3M2e-ferritin nanoparticle induced balanced Th1/Th2 immune responses, a long-term humoral response, and long-lived M2e-specific lymphocytes [30]. Intranasally administered 3M2e-ferritin nanoparticles induced a predominantly secretory IgA at the mucosal surfaces and fully protected the immunized mice against challenges by lethal homosubtypic human H1N1 and heterosubtypic H9N2 avian influenza viruses.

1.2 Advantages of nanoparticle vaccine platforms in the development of influenza vaccine

1.2.1 The safety of nanoparticle vaccines

To apply a vaccine in clinical use, guaranteeing safety for the immunized population is critical. A stricter discipline related to vaccine development was applying to older adults and young children [31, 32]. Current inactivated virus vaccine candidates were from egg or cell-based production, and the whole influenza viruses were harvested and inactivated by formaldehyde[33]. The production

flow allowed the possibility that egg-allergic patients were sensitive to this type of vaccine [34]. Meanwhile, the split and whole inactivated influenza virus vaccine still possess potential risk because of the replication possibility of the retained influenza virion genome. The fusion proteins or peptides were secreted or anchored by host cells and thus avoid containing egg components. New nanoparticle vaccines only consist of pure fusion proteins or peptides, with no virion DNA or RNA. For example, a very common baculovirus system can be used in expressing recombinant M2e based virus-like particles[28]; co-assembling peptides (CAPs) spontaneously assembled to a nanoparticle by the interaction of hydrophobic and hydrophilic residues[35]. These two strategies provide a safe route to make a particle without viral genomes.

1.2.2 Reducing the complexity of designing a nanoparticle

In the generation of nanoparticles from protein modules, each nanoparticle possesses its own process flow or protocol for production. From the point of the production complexity, fabricating polymer-based or desolvated nanoparticles is easier than VLPs and self-assembly nanoparticles. To construct VLPs or self-assembly nanoparticles, several factors should be considered during designing. (1) Whether the chimeric VLP protein can be secreted by host cells. Hence, to successfully construct the influenza VLP, researchers usually adapted M1 from the influenza virus as the intracellular domain and thus limited the antigen combination. (2) Whether the peptide can be self-folded to a protein nanoparticle. To form a symmetry pattern, fusion proteins of two oligomerization domains preferring a-helical conformation should be held together at a right angle and in a rigid fashion [36]. When designing a self-assembly peptide, researchers should consider the structure of amino acids from influenza antigen and obey the roles of constructing peptide-based building blocks into discrete morphologies [37].

The novel physicochemical-driven protein nanoparticle vaccines adapted the following manufacturing strategy: (1) concentrating a protein solution with polar solvents (such as ethanol) to form a particulate protein core; and (2) crosslinking other proteins onto the core by using a reversible crosslinker such as 3,3'-Dithiobis(sulfosuccinimidylpropionate) (DTSSP) [38]. In this study, two distinct proteins (Neuraminidase and M2e protein) with natural structures have been expressed and crosslinked by using this strategy.

1.2.3 Effectively displaying neuraminidase and M2e antigen in layered protein nanoparticles

Core/shell layered protein nanoparticles effectively display antigens in two aspects: a. increase the number of authentic neuraminidase and M2e antigen molecules in nanoparticles; b. broaden the antigen combination of influenza antigens.

a. One of the current self-assembly nanoparticles adapted ferritin as the core structure protein to load the influenza antigen. However, the non-specific effect (off-target) of the vaccine was induced because a significant antibody level against ferritin can be found in immunized mice. [39]. Our novel physicochemical-driven protein nanoparticles consist of two natural antigens (Neuraminidase and M2e protein), which avoid introducing the exogenous protein and prevent the off-target effect.

b. Most proteins in solution can be desolvated by adding desolvation reagents such as natural salt or organic solvent (methanol, ethanol, etc.): the proteins solute could aggregate into nanoparticles after removing the original solvent [40]. Because the naked desolvated protein nanoparticles can further crosslink with different proteins sequentially on their surfaces, multiply layered protein nanoparticles can be fabricated to accommodate different antigens for differential antigen-processing and presentation for a synergistic immune response. In other words, these two antigens in nanoparticles are convertible: either M2e core or coated neuraminidase can be switched to other

antigens from influenza virion, and the combination is arbitrary. Thus, the layered protein nanoparticles broaden the antigen combination pool and increase the number of possible influenza vaccine candidates.

1.2.4 Extended storage period at room temperature

Vaccine storage is one crucial issue for maintaining antigen immunogenicity. Usually, in high-income countries, the cold chain industry is mature and well developed. However, in many low-income countries, the need for storage is not optimal because of the shortage of electricity and insufficient funding for cold chain equipment [41].

The layered protein nanoparticles improved the storage time. The influenza-based hemagglutinin (H7) nanoparticles maintained the intact shape and size to more than 3 months at 25°C. Such nanoparticles were also stable for 2 weeks at 37°C. Moreover, the warm-aged nanoparticle did not lose hemagglutinating activity and thus induced high anti-HA titer in boost-immunized mice as in the fresh nanoparticle group [42]. With this stability, the physicochemical-driven protein nanoparticles would be a promising vaccine technic to low-income countries outside of the cold chain.

1.3 Microneedle patches encapsulating flagellin-adjuvanted nanoparticles

1.3.1 The application of flagellin in vaccine development

FliC is the major structural protein of Gram-negative bacteria flagella and a potent adjuvant [43]. Toll-Like Receptor 5 (TLR-5) recognizes FliC and initiates an innate signaling cascade. The consequence includes the generation of transcription factor NF-κB and subsequent gene expression, such as TNF-α. Previous studies have added FliC to different antigen combinations to increase dendritic cell (DC) cytokine and chemokine production, maturation, and antigen-processing/presentation. FliC could also enhance the protection breadth of the influenza vaccines.

For example, while H1/M1 VLPs conferred no protection to H3N2, FliC-adjuvanted H1/M1 VLPs effectively improved heterosubtypic protection against H3N2 [44-46]. We have expressed 4M2e-tFliC and 4M2e-HA stalk fusion proteins as standalone vaccines or as supplements to improve the immunity breadth of inactivated vaccines [38].

However, a high dose of a flagellin-M2e fusion protein (STF2.4×M2e) vaccination generated an overproduction of inflammatory molecules in a clinical trial [47]. Conversely, a lower amount (0.5 μg) of FliC-adjuvanted HIV VLPs induced significantly higher levels of neutralizing antibody responses than non-adjuvanted VLPs without abnormal symptoms seen [48]. In the present work, we are using a flexible and controllable DTSSP crosslinking method to introduce FliC onto the surface of the M2e core nanoparticles to enhance immune responses while minimizing the side effects of FliC.

1.3.2 The advantage of the application of microneedle patches

Microneedles are a new delivery platform for drugs, including vaccines targeting skin administration. This technology delivers immunogens directly to dendritic cells and epidermal Langerhans cells in the epidermis and dermis [49]. After absorbing immunogens, dendritic cells in the dermis migrate to draining lymph nodes and activate the expansion of T cells [50]. Langerhans cells in the dermis cross-present immunogens and have anti-tumor and anti-viral roles [51]. Skin vaccination by microneedle patches has displayed many advantages over traditional intramuscular vaccination and is an improved delivery method. Skin vaccination focuses on antigen-presenting cells by delivering immunogens to T cells or B cells near draining lymph nodes. Compared to intramuscular vaccination, microneedle patches enlargen the contact surface of immunogens and immune cells and increase immune efficiency. Finally, immunization by

microneedles is significantly less painful than intramuscular vaccination [52] and can be easily handled by healthcare providers or even by patients themselves [53].

Researchers have also studied encapsulating nanoparticles or VLP in microneedles in hopes of enhancing protection. Zaric et al. encapsulated PLGA with OVA and delivered these PLGA nanoparticles into the dermis of mice. The study demonstrated strong antigen-specific immune responses. Quan et al. stabilized PR8 VLPs in microneedles by adding trehalose disaccharide. These stabilized microneedles induced high titers of IgG2a and 100% protection against a lethal viral challenge, which was superior to intramuscular or unstabilized microneedles [54]. Moreover, microneedle delivered PR8 VLPs induced long-lasting (14 months after a single immunization) lung IgG and IgA responses, increased antibody-secreting splenocytes, and conferred protection to elderly mice [55]. Kim et al. constructed a tandem M2e repeat (M2e5x) VLP, which elicited IgG2a and IFN-γ secreting cell response and protected mice against heterosubtypic H1N1, H3N2, and H5N1 influenza virus challenges via a microneedle delivery route. The M2e-5x VLP dissolved microneedle was stable for eight weeks at room temperature [56]. In one of our recent studies, dissolvable microneedle patches encapsulated with NP polypeptide or NP protein nanoparticles demonstrated robust CD8+ T cell responses [57].

2 SPECIAL AIMS

Influenza, a type of negative-sense, single-stranded RNA virus, belonging to the family of *Orthomyxoviridae,* presented a real threat to public health annually. The current seasonal influenza vaccine confers only limited protection due to the antigenic shift and drift of major influenza surface antigens. A universal influenza vaccine that induces broad cross-protection against different viruses will negate annual vaccinations and protect against possible influenza pandemics. The extracellular domain (M2e) of the influenza matrix protein 2 (M2) contains a highly conserved amino acid sequence. Its 8 N-terminal amino acid residues (SLLTEVET) is over 99% conserved among all subtype A influenza viruses [25]; another influenza surface glycoprotein, neuraminidase (NA) contains highly conserved epitopes that have elicited universal anti-NA antibodies against all sub-types of influenza A [17].

A novel layered protein nanoparticle platform based on a core/shell orchestration is a highly potent vaccine platform. We found that M2e can be assembled into a particulate core by ethanal desolvation. A shell layer can be subsequently formed onto the core surface with influenza hemagglutinin (HA), or the globular head removed HA protein. Such double-layered nanoparticles induced broad protection against various viruses crossing different subtypes in mice [58]. In this study, we investigated whether a layered protein nanoparticle of M2e core/M2e-NA shell (designated M2e-NA Nano) can be constructed to induce broadly reactive immune responses in mice, functioning as a standalone or complementary component together with other immunogens in a future universal influenza vaccine. Moreover, skin vaccination with the FliC-adjuvanted NA/M2e nanoparticles by MNPs contributed to the generation of germinal centers, maturation of B cells, and induced robust humoral and cellular immune responses specific to M2e and NA. These

enhanced immune responses translated into broad cross-protection against the influenza viruses of homologous and heterosubtypic NA.

Aim 1: Determine whether enhanced protection will be conferred by M2e-NA Nano

1a: Generate and characterize M2e-NA Nano vaccines containing M2e and NA (four tandem repeat M2e and transmembrane domain removed NA protein)

1b: Determine the immunogenicity and protective efficacy of M2e-NANP vaccines in mice

Aim 2: Determine mechanisms of M2e-NANP in conferring protection in mice

2a: Determine the protective efficacy of M2e-NA Nano in heterosubtypic protection

2b: Determine detailed T cell responses of M2e and NA contributing to protection and efficacy

2c: Determine the impacts of novel vaccination on long-term protection

Aim 3: Determine the improved protection and immunological mechanisms of NA-FliC/M2e MNP induced protection in mice

3a: Determine whether NA-FliC/M2e nanoparticle (MFNA) can be incorporated to microneedle patches (MNPs)

3b: Determine the immunogenicity of MFNA MNP in mice

3c: Determine the protective efficacy of MFNA MNP in homogeneous and heterosubtypic protection

3 EXPERIMENT DESIGN AND RESULTS

3.1 Part I Double-layered M2e-NA Nanoparticles induce protection against divergent influenza viruses

3.1.1 Aim 1: Determine whether enhanced protection will be conferred by M2e-NA Nano

1a: Generate and characterize M2e-NA Nano vaccines containing M2e and NA (four tandem repeat M2e and transmembrane domain removed NA protein)

To fabricate effective immunogenic M2e-NA Nano, the selection of representative M2e or Neuraminidase is essential.

Rationale: (1) Currently, H1N1 and H3N2 influenza viruses are circulating in humans in flu seasons. Influenza neuraminidases have been divided into groups 1 with N1, N4, and N8 subtypes and group 2 covering N2, N3, N6, N7, and N9 [59]. Therefore, N1 and N2, the typical neuraminidases from two groups in phylogeny, can be chosen for the out-layer antigen of M2e-NA Nano.

(2) Compared to HA, M2e has weak immunogenicity. Researchers usually combine the epitope with higher immunogenic protein to overcome this weakness, like HA, or repeat the highly conserved sequence in tetrameric structures to increase the immunogenicity [27, 28]. In summary, as an excellent carrier, nanoparticles can be loaded with the conserved epitopes in the desired way for inducing a cross-protection against different subtypes of influenza viruses.

For the construction of the tetrameric M2e protein expressing vector, encoding sequences of a honeybee melittin signal peptide, a hexahistidine tag, a tetrameric motif tetrabrachion [60], and four tandem copies of different M2e were fused in-frame and subcloned into the transferring vector pFastBac for recombinant baculovirus (rBV) generation.

For the construction of the M2e-NA fusion protein-expressing vector, encoding sequences of neuraminidase 1 and 2 ectodomains [61] (N1 from A/Vietnam/1203/2004 (Viet, H5N1, Genbank Accession EF541467 (36H to 449K); N2 from A/Aichi/2/1968 (Aichi, H3N2, Genbank Accession AB295606 (38K to 469I)) were fused to the above tetrameric M2e encoding gene in-frame. The resulting tetrameric M2e-NA encoding genes were cloned into pFastBac and used to generate rBVs expressing M2e-NA fusion proteins.

We constructed genes encoding targeted conserved antigens (M2e, M2e-N1 fusion protein, and M2e-N2 fusion protein) (**Figure 1A**), generated recombinant baculoviruses (rBVs) with these genes, and expressed and purified the recombinant proteins in insect cells. Results from SDS-PAGE followed by the Coomassie blue staining and Western blotting analysis demonstrated that the proteins were purified to high purity, appearing as a major band in gel staining (**Figure 1B**), and the protein identities were confirmed by antigen-specific antibody detection in the Western blots (**Figure 1B**).

We generated M2e protein nanoparticles by ethanol desolvation as previously described [58]. In brief, the M2e core particles were formed by slowly adding a 4-fold volume of ethanol to a volume of M2e solution in PBS while stirring. The coating layer of M2e-NA fusion proteins was crosslinked onto the M2e cores using 3′-dithiol bis [sulfosuccinimidylpropionate] (DTSSP; Cat No. 21578, Thermo Scientific, Waltham, MA). After one and a half hours of incubation for the crosslinking reaction, the nanoparticle-containing supernatant was centrifuged at 15,000 rpm for 30 minutes. We collected the nanoparticle pellet, resuspended the pellet in PBS, and stabilized the nanoparticle suspension by sonication at a 40% amplitude on an iced-both. The size and surface potential of the layered M2e-NA protein nanoparticles were measured by dynamic light scattering (DLS) analysis with a Malvern Zetasizer Nano ZS (Malvern Instruments, Westborough, MA). Bis

[sulfosuccinimidyl] (BS3) crosslinking followed by the Western blotting analysis were performed to determine the polymeric state of the purified recombinant M2e and M2e-NA fusion proteins. A 10% SDS-PAGE followed with the Coomassie blue staining was applied for the characterization of the M2e-NA nanoparticle compositions. The ratio of M2e-NA to M2e protein was measured using GelQuantNET software after Coomassie blue staining. Monoclonal antibody 14C2 (Thermo Fisher Scientific, Cat. # MA1-082) was used for the confirmation of the M2e epitope in the M2e-NA nanoparticles.

Double-layered M2e-N1 or M2e-N2 nanoparticles were generated by coating M2e-N1 or M2e-N2 fusion proteins onto the surfaces of M2e nanoparticles with dithiobis (sulfosuccinimidyl propionate) (DTSSP) crosslinking (diagramed **Figure 1C**). The Coomassie blue staining and Western blotting analysis demonstrated the M2e and NA composition of the layered protein nanoparticles (**Figure 1D**). The size ranges of the resulting double-layered protein nanoparticles were 211.0 +/- 60.14 nm and 190.4 +/- 53.52 nm for M2e-N1 and M2e-N2 nanoparticles, respectively (**Figure 1F**, M2e-N1 Nano and M2e-N2 Nano). In comparison, the M2e core nanoparticle size was 176.4 +/- 48.3 nm (**Figure 1F**, M2e Nano). The layered M2e-N1 and M2e-N2 protein nanoparticles showed negative ζ-potentials of -27.77 +/-1.16 mV and -21.03 +/- 0.93 mV, and the loading ratios of M2e-N1 and M2e-N2 to the total protein in their layered protein nanoparticles were 62.1% +/- 2.5% and 59.3% +/- 1.8%, respectively. Neuraminidase activity assays showed the retention of NA activity in the resulting layered M2e-NA nanoparticles (**Figure 1E**). Transmission electron microscopy (TEM) observation further revealed the roughly spherical shape of the layered protein nanoparticles with irregular surfaces (**Figure 1G**).

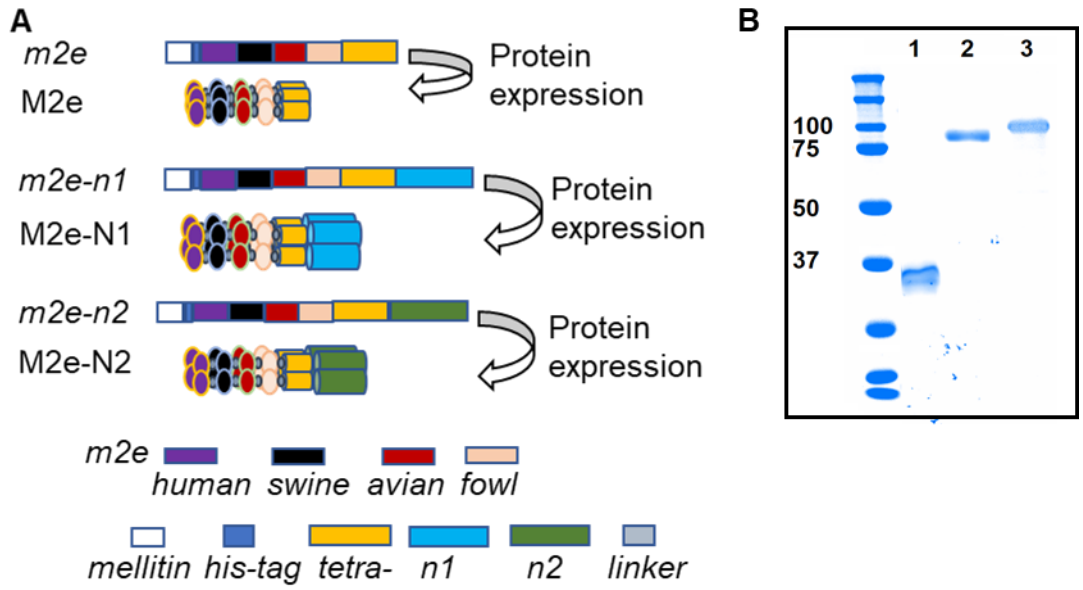
A
m2e
M2e
Protein expression
m2e-n1
M2e-N1
Protein expression
m2e-n2
M2e-N2
Protein expression
m2e
human swine avian fowl
mellitin his-tag tetra- n1 n2 linker
B
1 2 3
100
75
50
37

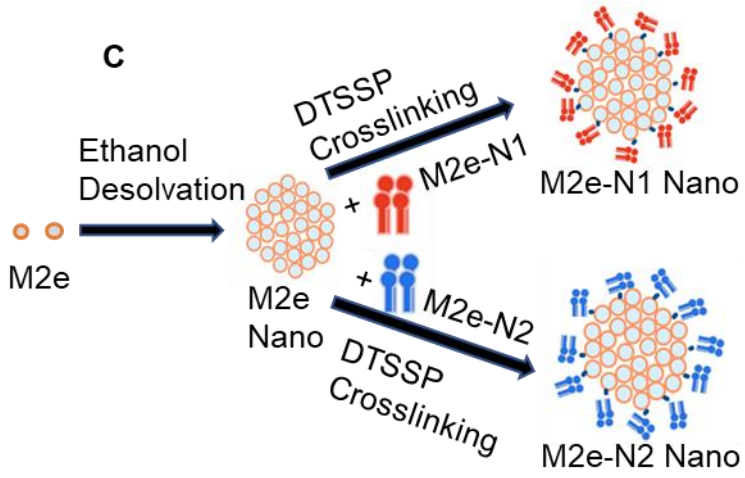
C
Ethanol Desolvation
M2e
M2e Nano
DTSSP Crosslinking
M2e-N1
M2e-N1 Nano
M2e-N2
DTSSP Crosslinking
M2e-N2 Nano

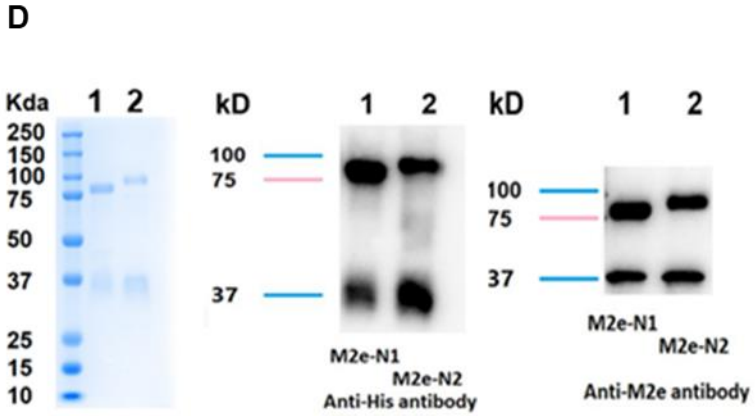
D
Kda 1 2
250
150
100
75
50
37
25
15
10
kD 1 2
100
75
37
M2e-N1
M2e-N2
Anti-His antibody
kD 1 2
100
75
37
M2e-N1
M2e-N2
Anti-M2e antibody

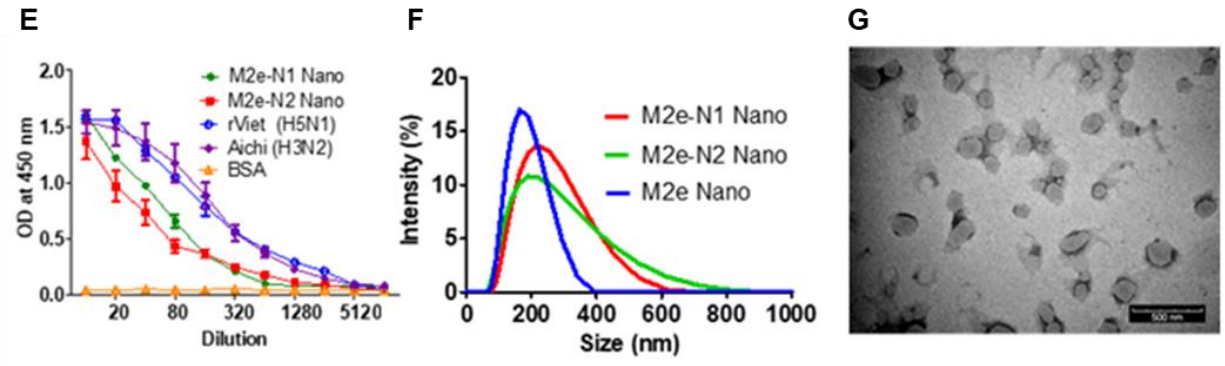

Figure 1. The fabrication of double-layered M2e-NA protein nanoparticles.
A. *Diagrams of M2e and M2e-NA fusion proteins and their coding sequence compositions. GS linker: glycine and serine GGSGGG; M2e: a recombination of four tandem M2e sequences from human, swine, avian, and domestic fowl influenza viruses stabilized by the tetrabrachion tetramerization sequence; M2e-N1 fusion protein: sequence of NA ectodomain (36H to 449K from Viet (H5N1) NA) fused with the four tandem M2e repeats and stabilized by the tetrabrachion sequence; M2e-N2 fusion protein: as M2e-N1 but the sequence of NA ectodomain is from Aichi (H3N2) NA(38K to 469I).* ***B.*** *Characterization of purified recombinant proteins with Coomassie blue staining. Line 1, recombinant M2e; Line 2, M2e-N1; Line 3, M2e-N2.* ***C.*** *Diagrams of layered protein nanoparticle generation. M2e protein nanoparticles (M2e Nano) were generated by ethanol desolvation. Double-layered M2e-N1 and M2e-N2 protein nanoparticles (M2e-N1 Nano and M2e-N2 Nano) were formed by crosslinking M2e-N1 and M2e-N2 fusion proteins onto the surfaces M2e Nano as coatings, respectively.* ***D.*** *Coomassie blue staining and western blotting of protein nanoparticles in a SDS-PAGE gel. Line 1, double-layered M2e-N1 protein nanoparticles; Line 2, double-layered M2e-N2 protein nanoparticles.* ***E****. Neuraminidase activity. NA activity was acquired by using ELLA as described in Materials and Methods. The concentration of M2e-N1 nanoparticle, M2e-N2 nanoparticle, Vietnam virus, or Aichi virus was 1mg/mL (total protein).* ***F****. The size range of protein nanoparticles. Red, M2e-N1 Nano; Green, M2e-N2 Nano; Blue, M2e Nano.* ***G.*** *TEM image of double-layered M2e-NA nanoparticles. All types of protein nanoparticles have a similar morphology. The image was acquired using double-layered M2e-N2 protein nanoparticles as an example. Bar scale, 500 nm.*

1b: Determine the immunogenicity and protective efficacy of M2e-NANP vaccines in mice

Six to eight-week-old BALB/c mice from Jackson Laboratory were used for the immunization and challenge experiments (n=5). There were five mouse groups for each M2e-NA nanoparticle group set: (1) PBS; (2) M2e-NA layered nanoparticle (10 μg total protein with ~6 μg of M2e-NA in the outer layer and ~4 μg of M2e in the core); (3) soluble M2e and soluble M2e-NA protein mixture (a dose of 10 μg total protein with 6 μg M2e-NA and 4 μg M2e); Mice received primary and boost

immunizations at a four-week interval by an intramuscular route. Immune sera were collected 21 days after the boost immunization.

Because the full-length NA will be loaded to the nanoparticles, it is of interest to investigate whether epitopes in NA or M2e protein will significantly activate the B cell response. Moreover, IFN-γ promotes the differentiation of Th1 CD4 T cells and thus increases the IgG2a secretion [62]; IL-4 increases the proliferation of Th2 CD4 T cells and promotes the IgG1 secretion [63]. Therefore, we want to examine whether the M2e-NANPs induce the correlated cellular immune response by specific NA or M2e epitopes.

Unlike the NA protein in live influenza viruses or inactivated vaccines, the NA fusion proteins on the surfaces of the layered protein nanoparticles were at high density and were not shielded by other larger immunogenic proteins, such as HA. We hypothesized that these traits made the NA fusion proteins highly immunogenic in the nanoparticles. Immune serum antibody titrations showed that the double-layered nanoparticle immunizations significantly increased NA and M2e-specific IgG antibody levels (the total serum IgG, as well as the IgG1 and IgG2a subtypes) compared with the soluble protein mixture immunization groups (sM2e+NA) (**Figure 2A** and **C**). Mice in the layered M2e-NA nanoparticle groups produced significantly higher M2e and NA-specific IFN-γ secreting splenocytes after the boost immunization (**Figure 2B** and **D**).

Because the neuraminidase inhibition (NAI) of immune sera is a correlate of NA mediated immune protection, we performed an NAI test to show the neutralizing ability of immune sera from every group[64]. Sera from the layered M2e-N1 nanoparticle and M2e-N2 nanoparticle groups showed potent neutralization to both homologous and heterologous NA influenza viruses. The M2e-N1 nanoparticle immune sera showed a significant decrease in OD_{450nm} (indicating an elevated NAI) compared with the sM2e+N1 (soluble protein mixture) immune sera up to a 20,480-fold dilution.

The layered M2e-N2 nanoparticle sera showed a significant decrease up to a 32,000-fold dilution in OD_{450nm} compared with the corresponding soluble protein mixture or untreated N2 virus (Aichi, or A/Hong Kong/99 (Hong Kong, H9N2)) NA activity (**Figure 2E** and **F**). However, immune sera from layered M2e-N1 or M2e-N2 nanoparticle groups showed lower levels of NAI activity against the heterosubtypic NA influenza viruses. Layered M2e-N1 nanoparticle immune sera showed a significant decrease in OD_{450nm} compared with the untreated Aichi/68 virus NA activity down to a 640-fold dilution while M2e-N2 nanoparticle sera showed a significant decrease in OD_{450nm} compared with the untreated A/California/2009 (Cal, H1N1, the 2009 pandemic strain) virus NA activity down to only a 500-fold dilution (**Figure 2E** and **F**).

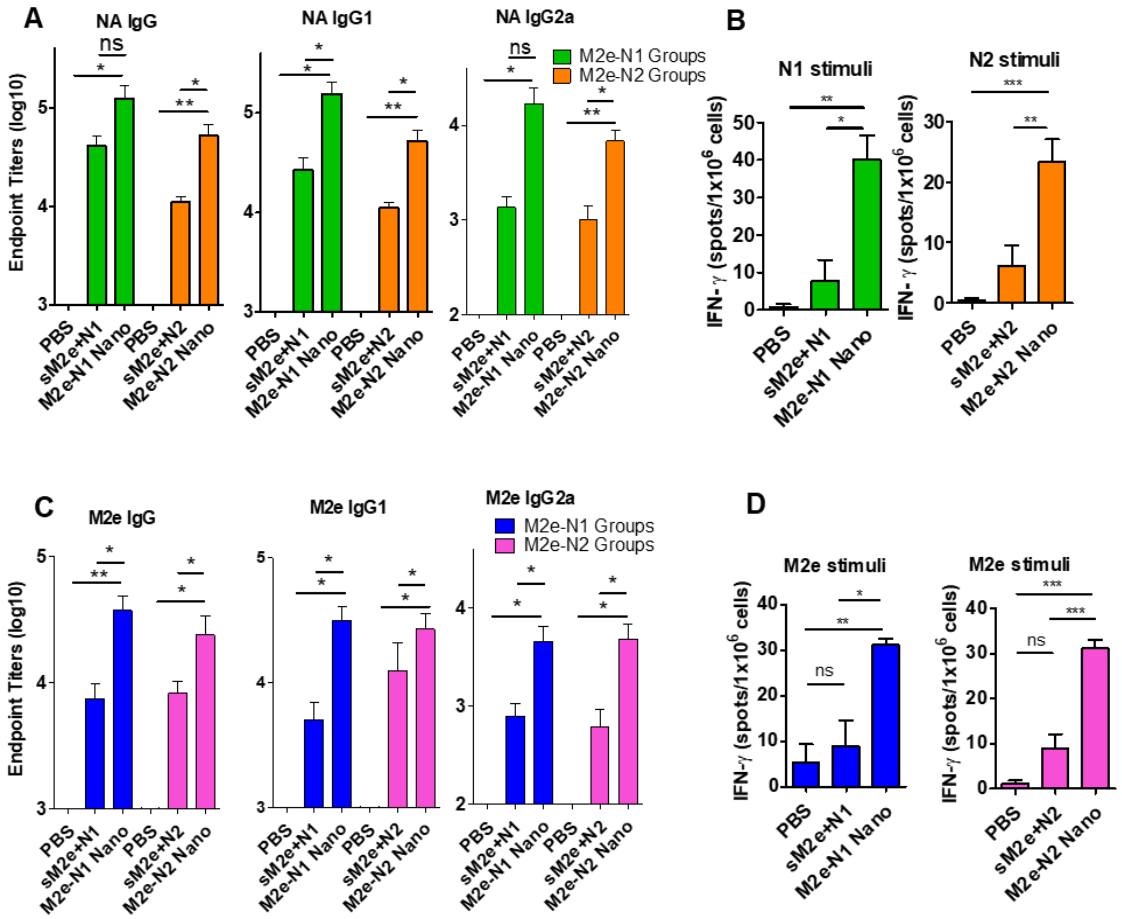

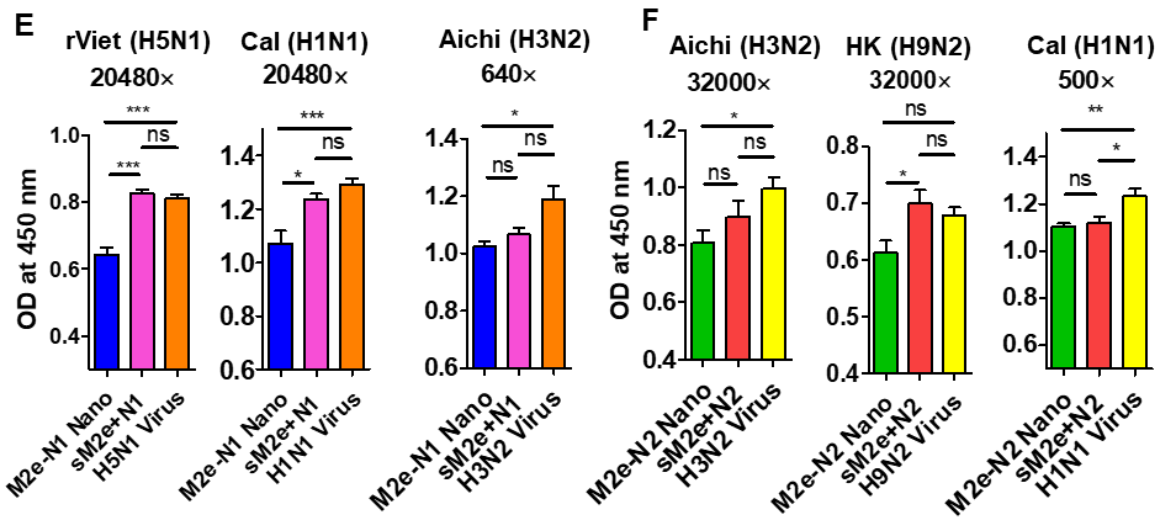

Figure 2. Humoral and cellular immune responses of vaccinated mice.

A. *Detection of NA-specific antibody responses by ELISA. Neuraminidase 1 (NA1) from Viet and Neuraminidase 2 (NA2) from Aichi were coated on the 96-well plates and sera from different groups were tested.* ***B****. Enumeration of NA-specific IFN-γ secreted splenocytes by ELISpot. The spleens of boost immunized mice were collected before the influenza challenge and N1 or N2 peptide pools were added to the homogenized splenocytes for stimulation.* ***C.*** *M2e-specific antibody responses. M2e peptide was coated on the 96-well plates and sera from different groups were tested for anti-M2e titers.* ***D****. Enumeration of M2e activated IFN-γ secreted splenocytes by ELISpot. The spleens of boost immunized mice were collected before the influenza challenge and M2e peptide pools were added to the homogenized splenocytes for activation.* ***E*** *and* ***F.*** *NAI test against different strains of influenza viruses. Sera from the M2e-N1 group set (****E****) were mixed with 8000 $TCID_{50}$ rViet (H5N1), Cal (H1N1), and Aichi (H3N2). The OD450 value was measured by using ELLA. The OD values have been compared with the virus only and naive serum reads. The end dilution titers of sera for the maximum significant inhibition are as follows: rViet (H5N1), 20480; Cal (H1N1), 20480; Aichi (H3N2), 640. Sera from the M2e-N2 group set (****F****) were mixed with 8000 $TCID_{50}$ Aichi (H3N2), Hong Kong (HK, H9N2), and Cal (H1N1). The end dilution titer of sera for the maximum significant inhibition is as follows. Aichi (H3N2): 32000, Hong Kong (H9N2): 32000, Cal (H1N1): 500. Data represent mean ± SEM. The statistical significance was analyzed by a two-tail unpaired t-test (n=5; *, $p < 0.05$; **, $p < 0.01$; ***, $p < 0.001$; ns, $p > 0.05$).*

We challenged mice in the layered M2e-N1 nanoparticle group with doses of 3× LD_{50} of the reassortant A/Vietnam/1203/2004 (rViet, H5N1, PR8 backbone with HA and NA from Viet), or 5× LD_{50} Cal and mice in the M2e-N2 nanoparticle group with doses of 5× LD_{50} of Aichi (H3N2) or Hong Kong (H9N2) viruses to verify immune protection against homologous or heterologous viral infection (**Figure 3**). Mice receiving the M2e-N1 or M2e-N2 nanoparticle immunizations completely survived their respective NA virus challenges (**Figure 3A** and **B**). Mice receiving the

soluble sM2e+N1 immunization had a 100% survival rate against the rViet challenge, but the sM2e+N2 immunization demonstrated partial protection against the homologous viral challenge (**Figure 3A** and **B**). The nanoparticle immunization groups tended to lose less bodyweight than the soluble protein immunization groups, with the Hong Kong (H9N2) viral challenge being an exception (**Figure 3**).

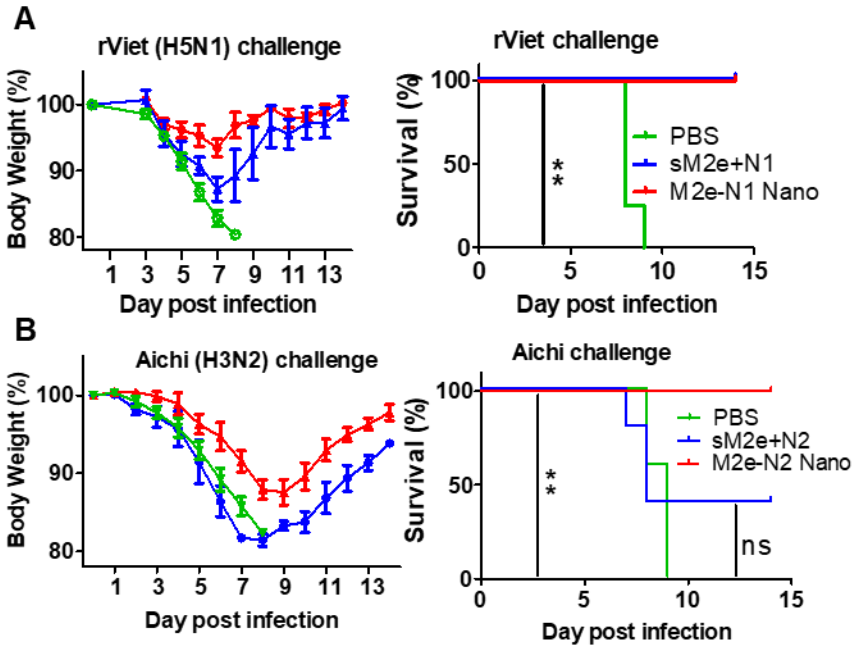

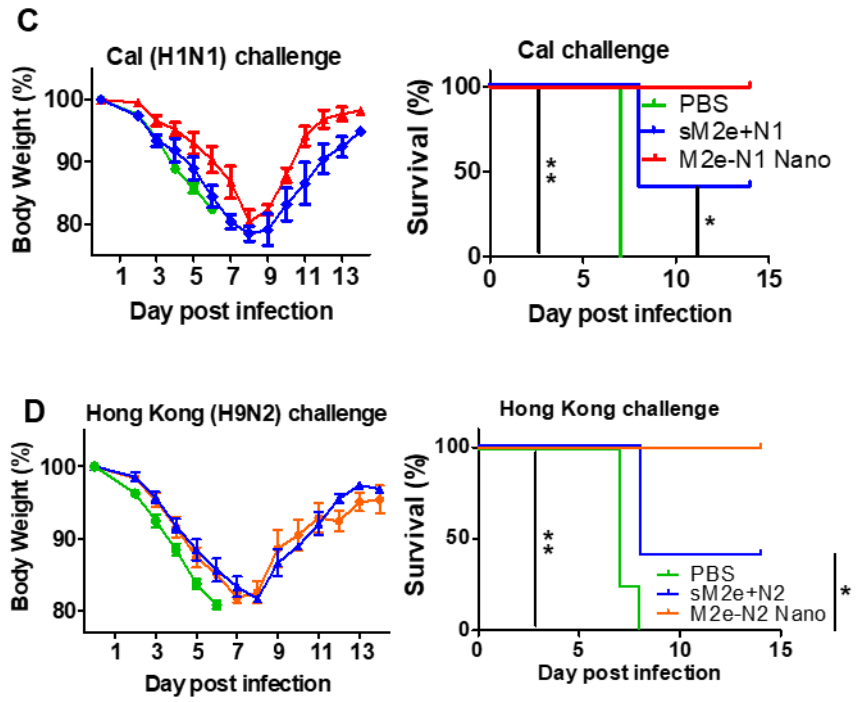

Figure 3. Immune protection against homologous and heterologous NA virus challenge. *A. Bodyweight monitoring and survival rate of M2e-N1 group set against the challenge of 3×LD_{50} rViet (H5N1); **B**. Bodyweight monitoring and survival rate of M2e-N2 group set versus 5×LD_{50} Aichi (H3N2) challenge. **C.** Bodyweight monitoring and survival rate of M2e-N1 group set versus 5×LD_{50} Cal (H1N1) challenge, **D.** Bodyweight monitoring and survival rate of M2e-N2 group set versus 5×LD_{50} Hong Kong (H9N2) challenge. Data represent mean ± SEM. The difference in survival rates between different groups was analyzed by Graphpad Prism, using the Log-rank test. (n=5; *, $p < 0.05$; **, $p < 0.01$; ns, $p > 0.05$).*

Furthermore, the layered protein nanoparticle immunization groups had significantly reduced viral titers in the lungs compared with the soluble protein groups five days after the homologous viral challenges. (**Figure 4A**). Histological examinations of the lung tissue from the challenged mice indicated that layered protein nanoparticle groups showed a lower degree of immune cell infiltration and inflammation near the alveolar walls compared to the sM2e-NA soluble protein mixture groups, but the naïve control mice presented a heavier inflammatory state and severe tissue damage (**Figure 4B**).

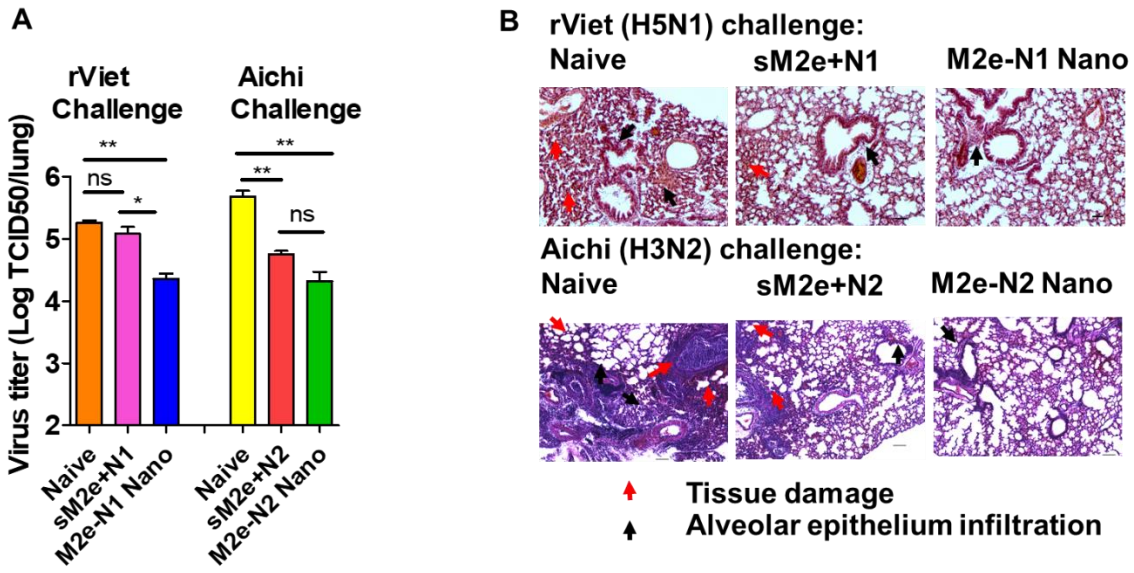

Figure 4. Lung viral titers and histology of M2e-N1 and M2e-N2 group sets.
A. *Viral titers of lungs from different immunization groups at 5 days after the infection.* ***B.*** *Histology examination by using H&E staining. Arrows show tissue damage and alveolar epithelium infiltration. Data represent mean ± SEM. The statistical significance was analyzed by the two-tail unpaired t-test. (n=5; *, $p < 0.05$; **, $p < 0.01$; ***, $p < 0.001$; ns, $p > 0.05$.)*

3.1.2 Aim 2: Determine mechanisms of M2e-NANP in conferring protection in mice

2a: Determine the protective efficacy of M2e-NA Nano in heterosubtypic protection

There was low NAI against heterosubtypic influenza strains in previous studies [65], here we included the M2e antigen to enhance the heterosubtypic protection. We have found that protein nanoparticles with M2e inner cores triggered strong T cell immune responses contributing to the overall cross-protective immunity. The protein nanoparticles of conserved influenza antigens preferentially induced non-neutralizing antibody responses [58]. The protection upon the passive serum transfer indicated that the M2e-specific antibody responses might confer protection via antibody-dependent cytotoxicity (ADCC) and antibody-dependent phagocytosis (ADPC), as previously observed [66].

We tested the cross-protection of the nanoparticles against heterosubtypic virus challenges. Because NA fusion proteins in this study are derived from N1 in Viet (H5N1) and N2 in Aichi (H3N2), $3\times LD_{50}$ of A/Philippines/2/82 (Philippines, H3N2) was applied to the M2e-N1

nanoparticle immunization cohort while 5×LD_{50} of Cal (H1N1) was applied to the M2e-N2 nanoparticle immunization cohort to test the heterosubtypic protection. Immunized mice in the M2e-N1 nanoparticle group showed a 100% survival against the Philippines virus challenge while the sM2e+N1 soluble protein mixture induced partial protection (**Figure 5A**). M2e-N2 nanoparticle immunized mice showed a 60% survival against the Cal virus challenge while mice from the corresponding sM2e+N2 soluble protein group, as well as naïve mice, reached their endpoints at day 7 post the challenge infection (**Figure 5B**).

5 mice from each group received the prime and boost immunization as described previously. After the boost immunization, mice serum from 4 groups in M2e-N1 or M2e-N2 team will be collected. Serum from different groups has been mixed with the same volume of H1N1 or H3N2 influenza virus and incubated on the 96-well plate with Fetuin and the Neuraminidase inhibition test was performed.

Passive transmission of immune sera can show the immunological role of the antibodies without T cell responses. To verify whether the immune sera from the M2e-NA nanoparticle group confer cross-protection against heterologous influenza viruses, we intraperitoneally injected naïve mice with 300 μL sera from double-layered protein nanoparticle-immunized mice 24 hours before the challenge infection. Sera from M2e-N1 nanoparticle and M2e-N2 nanoparticle immunized mice conferred enhanced protection against rH5N1 and H3N2 influenza virus infection as shown by 100% survivals and preventing severe body weight loss, respectively (**Figure 6C**, M2e-N1 Nano; **Figure 6D**, M2e-N2 Nano). Meanwhile, immune sera from sM2e+N1 and sM2e+N2 soluble protein-immunized mice showed weaker protection than their corresponding layered protein nanoparticles, demonstrated by significantly more severe morbidity in the soluble protein mixture groups upon challenge (**Figure 6C**, sM2e+N1; **Figure 6D**, sM2e+N2). These results demonstrated

that serum antibody responses contributed to the heterosubtypic protection in the layered protein nanoparticle immunization.

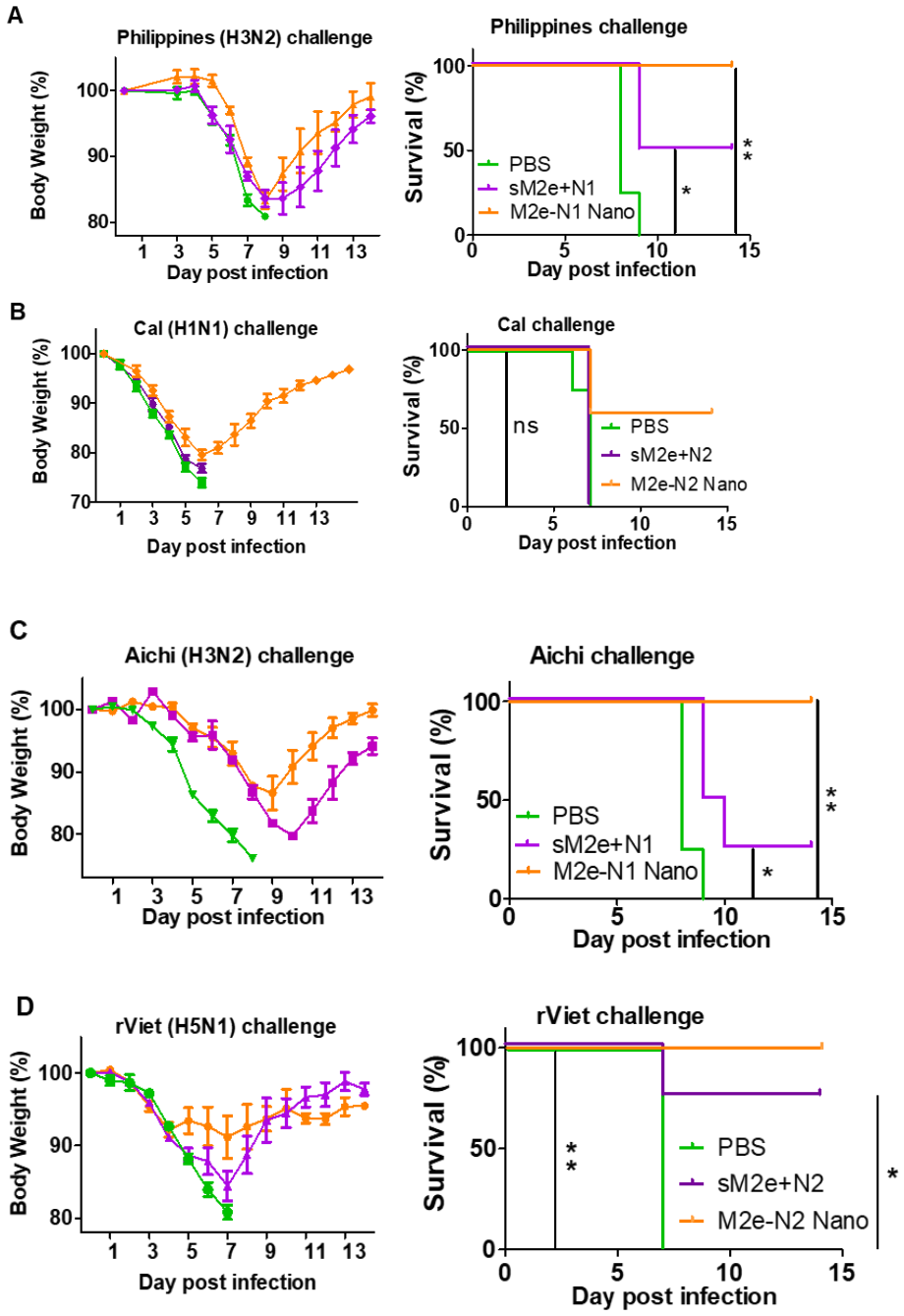

Figure 5. Immune protection against heterosubtypic NA virus challenge.
A. *M2e-N1 group set versus the challenge of 5×LD_{50} Philippines (H3N2).* ***B.*** *M2e-N1group set versus the challenge of 5×LD_{50} Cal (H1N1).* ***C*** *and* ***D,*** *body weight changes of mice upon passive immune serum transfers. Immune sera (300 μL) from layered M2e-N1 protein nanoparticle or sM2e+N1 immunized mice were I.P. injected into mice 24 hours before the challenge infection with 3×LD_{50} Aichi (**C**). Immune sera (300 μL) from layered M2e-N2 protein nanoparticle or*

*sM2e+N2 immunized mice were I.P. administered to mice 24 hours before the 3×LD_{50} rViet challenge infection (**D**). Bodyweight changes were monitored for 14 days post the challenge.*
*Data represent mean ± SEM. The statistical significance of survival rate was analyzed by Graphpad Prism, using the Log-rank test (n=5; *, p < 0.05; **, p < 0.01; ns, p > 0.05.)*

2b: Determine detailed T cell responses of M2e and NA contributing to protection and efficacy

NA has been known to induce both CD4 and CD8 T cell responses[67]. Upon influenza infection, both $CD8^+$ CTL and $CD4^+$ helper T cells differentiate and proliferate into effector cells with the increasing IFN-γ secretion [68]. In our previous studies, we have found protein nanoparticles with M2e inner cores triggered strong T cell immune responses contributing to the overall cross-protective immunity [58]. Thus, we want to further investigate the T cell responses to NA or M2e. We compared different T cell responses induced by double-layered M2e-NA nanoparticles and sM2e+NA protein mixtures. CD4 T cells facilitate B cell differentiation and maintenance of CD8 cytotoxic T cell response, while CD8 T cells have a role in viral clearance from the lungs [69]. The layered M2e-N1 nanoparticle immunization significantly increased the number of IFN-γ secreting CD4 and CD8 T cells in the lungs five days after the rViet (H5N1) infection (**Figure 6A**, **B**, **E,** and **F**). The layered M2e-N2 nanoparticle immunization induced even stronger T cell responses, demonstrated by higher numbers of IFN-γ secreting CD4 and CD8 T cell populations in the lung five days after the Aichi (H3N2) challenge infection (**Figure 6C**, **D**, **E,** and **F**). In contrast, the soluble protein mixture immunization did not show significant T cell population activation upon the challenge infection of homologous NA influenza viruses (**Figure 6A** and **B**, sM2e+N1 *verse* the rViet challenge; **Figure 6C** and **D**, sM2e+N2 *verse* the Aichi challenge).

To investigate whether the CD8 T cell responses correlate with the immune protection, we depleted CD8 T cells from M2e-NA nanoparticle immunized mice by injecting 300 μL anti-CD8 antibody clone 2.43 (Cat no. BE0061; BioXCell) 24 hours before and after the challenge infection. CD8 T cell depletion groups showed a greater body weight loss and a decreased survival rate over

immunized groups without the depletion (**Figure 6G** and **H**). We observed that double-layered M2e-NA protein nanoparticles increased the populations of effector T cells secreting IFN-γ. The protection of M2e-NA nanoparticle-immunized mice was impaired after CD8 T cell depletion - demonstrating M2e and NA-specific CTL responses contribute to the protection observed in the study. We concluded that NA-specific T cell responses, in addition to M2e T cell responses, played an important role in the protein nanoparticle-induced cross-protection. These results indicated that layered M2e-NA protein nanoparticles conferred immune protection at least partially through CD8 T cell responses against influenza infection.

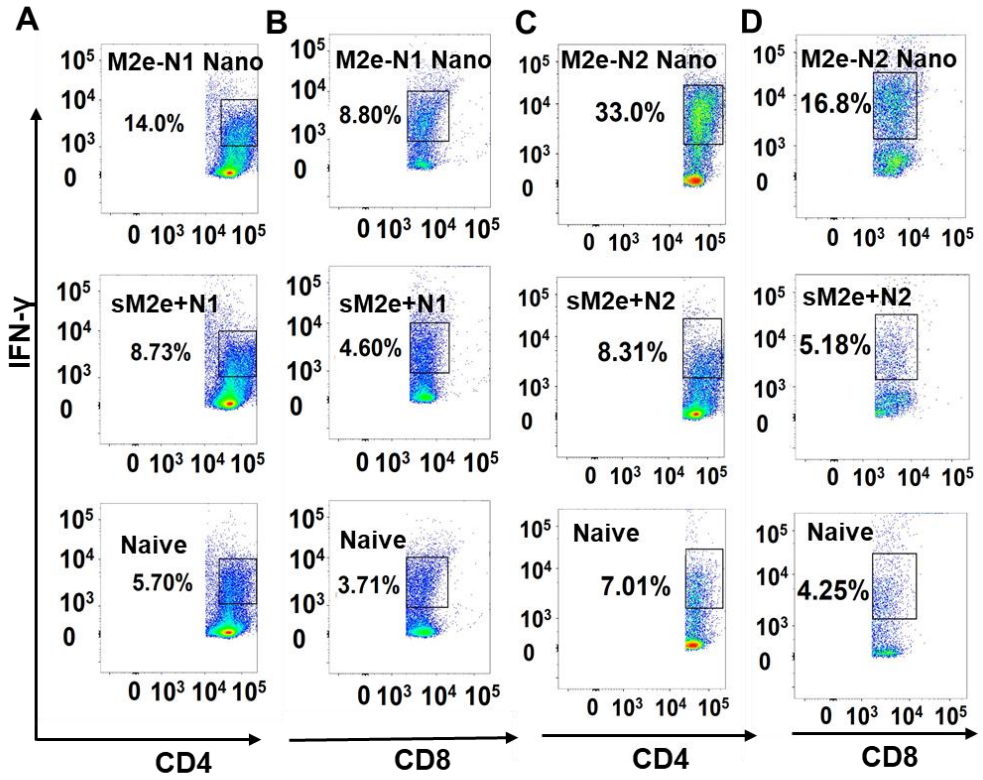
A
B
C
D
M2e-N1 Nano
14.0%
M2e-N1 Nano
8.80%
M2e-N2 Nano
33.0%
M2e-N2 Nano
16.8%
sM2e+N1
8.73%
sM2e+N1
4.60%
sM2e+N2
8.31%
sM2e+N2
5.18%
Naive
5.70%
Naive
3.71%
Naive
7.01%
Naive
4.25%
IFN-γ
CD4
CD8
CD4
CD8

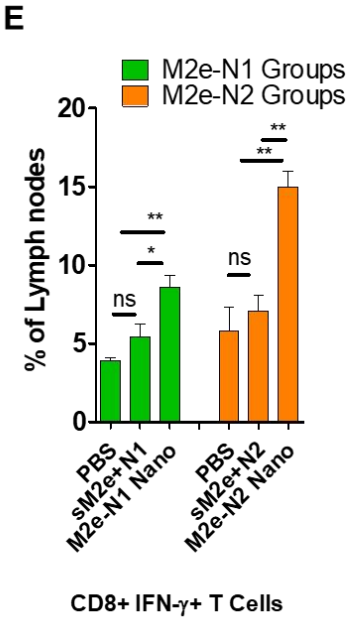
E
M2e-N1 Groups
M2e-N2 Groups
% of Lymph nodes
ns
ns
PBS
sM2e+N1
M2e-N1 Nano
PBS
sM2e+N2
M2e-N2 Nano
CD8+ IFN-γ+ T Cells

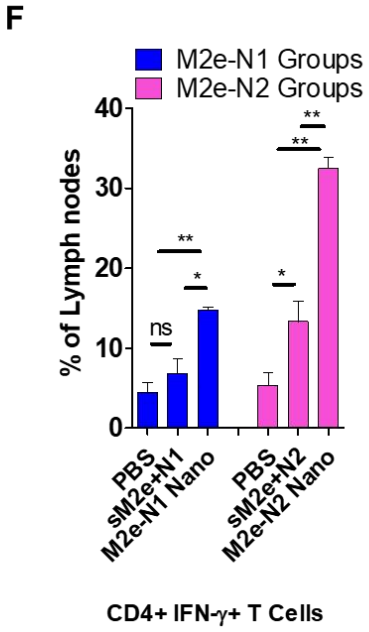
F
M2e-N1 Groups
M2e-N2 Groups
% of Lymph nodes
ns
PBS
sM2e+N1
M2e-N1 Nano
PBS
sM2e+N2
M2e-N2 Nano
CD4+ IFN-γ+ T Cells

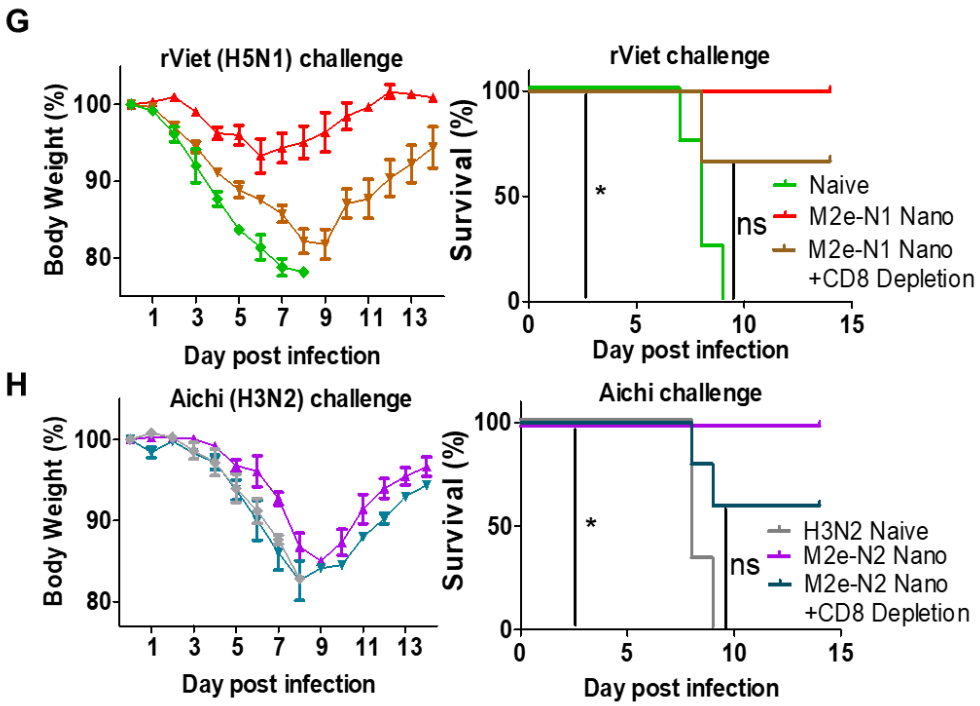

Figure 6 T cell responses in M2e-NA nanoparticle immunized mice.
Characterization of T cell response by selected cell markers with FACS. After stimulation by N1 or N2 peptides, the homogenized lung cells were stained by antibodies against CD3, CD45, CD4, CD8, and intracellular cytokines IFN-γ. Lymphocytes were marked by selecting CD3, CD45+ gated cells. ***A.*** *CD4+, IFN-γ+ T cells;* ***B.*** *CD8+, IFN-γ+ T cells. Cells were stimulated with an N1 peptide pool.* ***C.*** *CD4+, IFN-γ + T cells;* ***D.*** *CD8+, IFN-γ+ T cells. Cells were stimulated with an N2 peptide pool.* ***E, F.*** *Percentages of INF-γ-secreting CD8 T cells (**E**) and CD4 T cells (**F**) were acquired from flow cytometry data in* ***Figure 6A*** *to* ***D****.* ***G.*** *T cell depletion assay of M2e-N1 nanoparticle immunized mice versus 3×LD_{50} H5N1.* ***H.*** *T cell depletion assay of M2e-N2 nanoparticle immunized mice versus 5×LD_{50} H3N2. Data represent mean ± SEM. The statistical significance was analyzed by the two-tail unpaired t-test, and the survival rate between different groups was analyzed by Graphpad Prism, using Log-rank test (Num=5, * $p < 0.05$, ** $p < 0.01$, ns $p > 0.05$.)*

2c: Determine the impacts of novel vaccination on long-term protection

When developing a vaccine, scientists expect more about persistent efficacy. Moreover, elder people are susceptible to influenza infection because of immunosenescence [70]. Therefore, a long-lasting immune response is a necessary feature for an ideal vaccine. Here, we evaluated the longevity of the immunity induced by the double-layered protein nanoparticle formulations. We immunized mice with M2e-N1 nanoparticles, M2e-N2 nanoparticles, or soluble M2e and M2e-NA proteins twice with a 4-week interval. After four months, we collected the immune sera from

the mice. Immunized mice in both double-layered M2e-NA protein nanoparticle groups maintained significantly higher M2e- and NA-specific antibodies than the soluble protein mixture groups (**Figure 7A** and **B**).

We then challenged the layered M2e-N1 protein nanoparticle-immunized mice with rViet (H5N1) and the layered M2e-N2 protein nanoparticle-immunized mice with Aichi (H3N2). The immune protection of the nanoparticle group was unchanged against the viral challenges up to 4 months after the immunizations. Furthermore, the double-layered protein nanoparticle immunizations limited morbidity significantly than the soluble protein immunizations (**Figure 7C** and **D**).

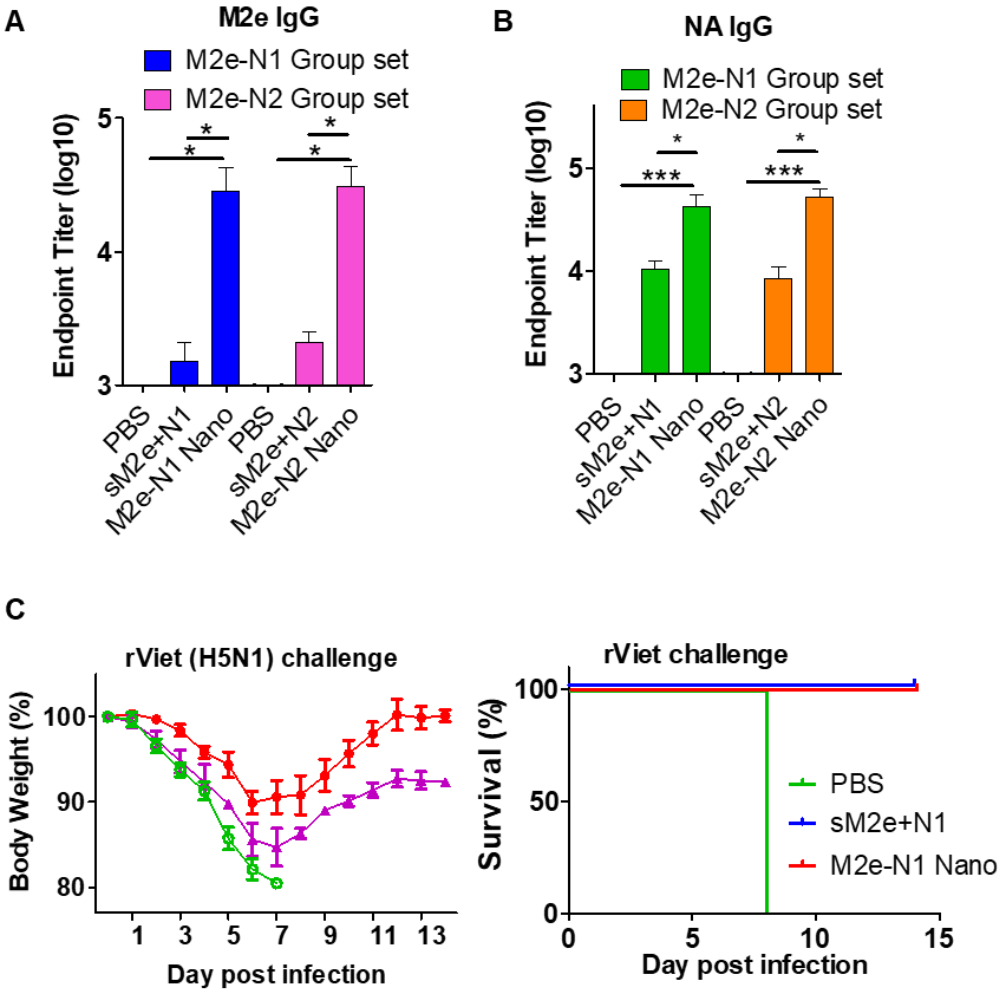

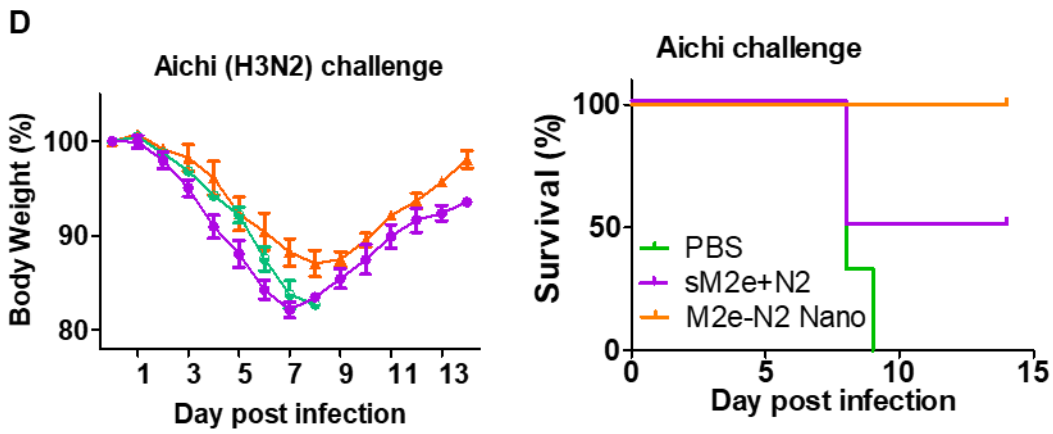

Figure 7. Long-term immune protection.
A *and* ***B.*** *long-term antigen-specific antibody binding titers. M2e-specific (****A****) and NA-specific* ***(B)*** *antibody titers in immune sera from mice 4 months after boost immunizations were measured by ELISA.* ***C*** *and* ***D.*** *Long-term immune protection. M2e-N1 group set was challenged with 3×LD_{50} rViet 4 months after the boost immunization (****C****). M2e-N2 group set was challenged with 3×LD50 Aichi 4 months after the boost immunization (****D****). Data represent mean ± SEM. The statistical significance was analyzed by the two-tail unpaired t-test, and survival rates were analyzed by Graphpad Prism, using Log-rank test (n=5; *, p < 0.05; **, p < 0.01; ***, p < 0.001; ns, p > 0.05.).*

3.1.3 Conclusion

In conclusion, the double-layered M2e-NA protein nanoparticles were highly immunogenic, inducing broadly reactive immune responses against both M2e and different NA antigens. The induced immunity conferred protection against viruses of different NA subtypes. Both antibody and T cell immune responses contributed to cross-protection. Our results showed that double-layered M2e-NA protein nanoparticles had the potential to be developed into influenza universal vaccines, either alone or as a synergistic component in more complicated influenza universal vaccine formulations. The incorporation of stabilized antigenic proteins into layered protein nanoparticles could be a general vaccine strategy for different pathogens.

3.2 Part II Skin vaccination with dissolvable microneedle patches incorporating influenza neuraminidase and flagellin protein nanoparticles induces broad immune protection against multiple influenza viruses

3.2.1 Aim 3: Determine the improved protection and immunological mechanisms of NA-FliC/M2e MNP induced protection in mice

3a: Determine whether NA-FliC/M2e nanoparticle (MFNA) can be incorporated to microneedle patches (MNPs)

For Neuraminidase (NA) construction, a honeybee melittin signal peptide, a tetrameric motif tetrabrachion, and hexahistidine tag were preserved from the previous M2e-NA nanoparticle project [71]. The sequences of transmembrane removed Neuraminidase 1 and 2 were followed behind the tetrabrachion sequence. For the M2e protein expression vector, we kept the previous construct as in the M2e-NA nanoparticle project [71]. For FliC gene construction, the flagellin gene (*fliC*; GenBank accession no. D13689) was ligated into the pet-22b(+) vector. (**Figure.1.A**) After the generation of recombinant baculoviruses (rBVs) encoding the extracellular domain of M2 (M2e), neuraminidase1 (NA1), and neuraminidase2 (NA2), the M2e, NA1, and NA 2 protein have been expressed and purified. The FliC protein was also purified from a bacterial protein expression as previously described [38]. The purified NA1, NA2, and FliC proteins showed major bands in the Coomassie Blue gel staining and Western blotting results, respectively (**Figure. 1B**). Previously, the FliC has been purified either in fused status with influenza antigen or co-expressed within virus-like particles (VLP) [38, 45]. DTSSP could crosslink its sulfo-NHS-ester to primary amines in the side chain of lysine (K) residues in FliC and M2e protein core [72]. Our lab successfully crosslinked the HA-FliC or M2e-FliC fusion protein onto the M2e core. The resulting self-adjuvanted nanoparticle fully protected mice from a lethal dose of influenza viral challenge

[38]. We fabricated double-layered N1-FliC/M2e and N2-FliC/M2e nanoparticles (designated as MFN1 and MFN2) by using the DTSSP crosslinking method as diagramed in **Figure.1C**. The Coomassie blue staining confirmed the M2e, NA, and FliC composition of the layered protein nanoparticles (Figure.1D, MFN1, MFN2). Protein components in double-layered nanoparticles were confirmed by using anti-His, FliC, or M2e antibodies (**Figure.1D**).

The resulting double-layered protein nanoparticles had particle sizes in a range of 150-250 nm (MN1, 195.8 +/- 26.2 nm; MN2, 213.4 +/- 27.6 nm; MFN1, 245.6 +/-20.5 nm; and MFN2, 223.5 +/- 15.6 nm. **Figure 1E**). The polydispersity index (PDI) of four nanoparticles is less than 0.2. All layered protein nanoparticles showed negative ζ-potentials: MN1, −27.76 +/−1.19 mV; MN2, −21.26 +/− 0.98 mV; MFN1, -26.5+/- 1.01 mV; MFN2, -22.36 +/- 0.43 mV. Transmission electron microscopy (TEM) observation revealed the roughly spherical shape of the layered protein nanoparticles (**Figure 1E**). MFN1, MFN2, or soluble FliC protein, stimulated 293T cells (with transfection of plasmids containing TLR5 and NF-κB-luciferase reporter genes) to produce comparable levels of TLR5 innate signal as demonstrated by their similar RLUs [73] (**Figure 1F**).

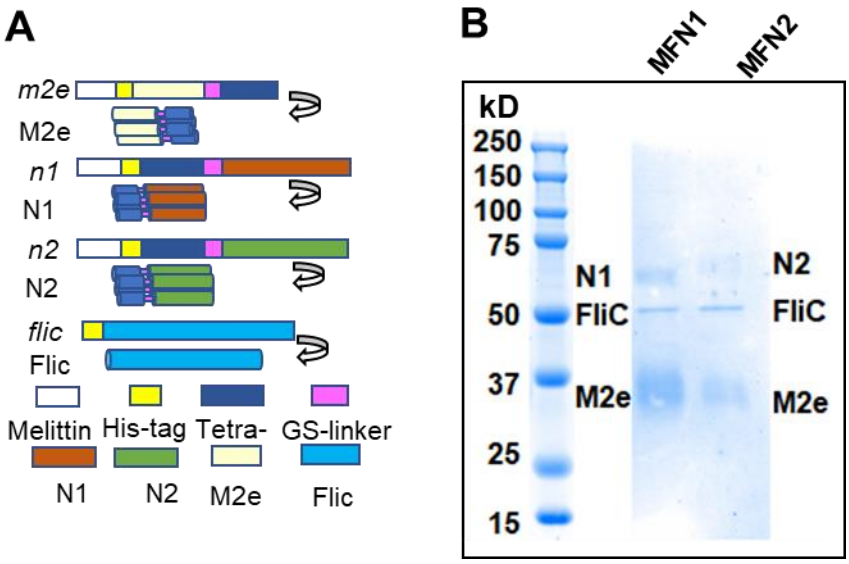

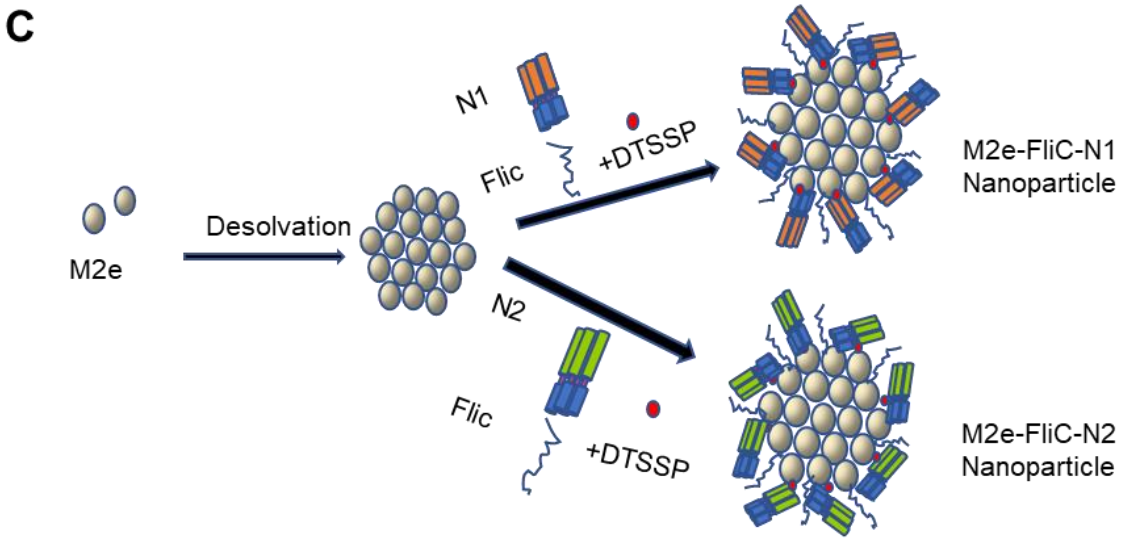
C
N1
Flic
+DTSSP
M2e-FliC-N1
Nanoparticle
Desolvation
M2e
N2
Flic
+DTSSP
M2e-FliC-N2
Nanoparticle

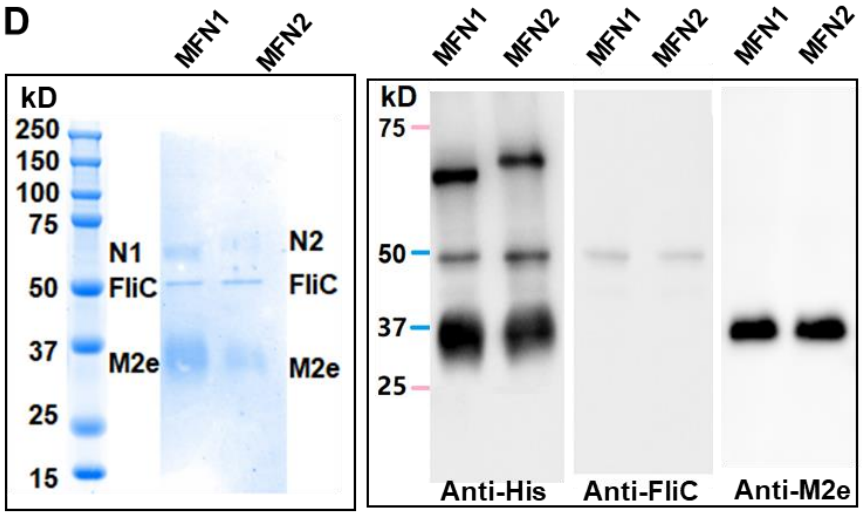
D
MFN1
MFN2
kD
250
150
100
75
50
37
25
15
N1
FliC
M2e
N2
FliC
M2e
MFN1
MFN2
MFN1
MFN2
MFN1
MFN2
kD
75
50
37
25
Anti-His
Anti-FliC
Anti-M2e

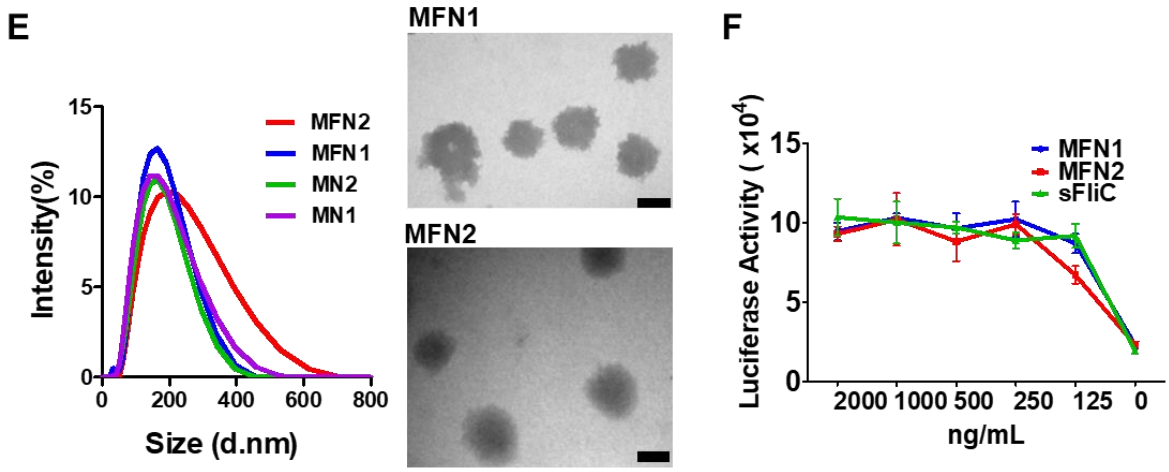

Figure. 1 The characterization of double-layered NA-FliC/M2e and NA/M2e protein nanoparticles.
A. *Diagrams of M2e, NA, and Flagellin fusion proteins and their coding sequence compositions. GS linker: glycine and serine GGSGGG; M2e: recombination of four tandem M2e sequences from human, swine, avian, and domestic fowl influenza viruses stabilized by the tetrabrachion tetramerization sequence; NA1 recombinant protein: the sequence of NA ectodomain (36H to 449K from Viet (H5N1) NA) fused and stabilized by the tetrabrachion sequence; NA2 recombinant protein: as NA1 fusion protein but the sequence of NA ectodomain is from Aichi (H3N2) NA (38K to 469I). FliC: the full-length fliC gene followed by 6x His-tag.*
B. *Coomassie blue staining of purified NA1 (N1), NA2 (N2), and FliC recombinant proteins.*
C. *Diagrams of layered MFN generation. M2e protein nanoparticles (M2e Nano) were generated by ethanol desolvation. Double-layered NA1-FliC/M2e- and NA2-FliC/M2e-protein nanoparticles (MFN1 and MFN2) were formed by crosslinking NA1, NA2, and FliC proteins onto the surfaces M2e core as coatings, respectively.* ***D.*** *Coomassie blue staining and Western Blot analysis of the fabricated MFN1 and MFN2 nanoparticles.* ***E.*** *Left panel, The size range of protein nanoparticles. Right panel, TEM images of MFN1 and MFN2. Bar scale: 200 nm.* ***F****. TLR5-specific bioactivity of MFN1, MFN2, and soluble FliC.*

The skin is the largest immune organ with high populations of dermal dendritic cells (DCs) [74, 75]. Our nanoparticles target skin dendritic cells for optimal DC maturation by MNP skin vaccination. We observed an increased fluorescence intensity in JAWS II cells - a dendritic cell line originated from mouse bone marrow - incubated with AF488-labeled MFN1 nanoparticles compared with a soluble protein mixture of AF488-labeled M2e, NA1, and FliC (designated sMFN1) (**Figure 2A**, MFN1 vs. sMFN1). MFN1 nanoparticles significantly increased the fluorescence intensity 1 hour after incubating with JAWS II cells. Meanwhile, the soluble protein-

treated group showed substantially fewer cells with positive AF488 signals (**Figure 2A**). These results demonstrate that DCs could effectively internalize double-layered protein nanoparticles.

We further evaluated whether protein nanoparticles induced DC maturation. Because IL-6 and TNF-α cytokines can trigger DC maturation via an autocrine fashion [76, 77], we measured the secretion levels of these two cytokines by JAWS II cell or primary bone marrow dendritic cells (BMDC) culture after treatments with different antigens. FliC significantly elevated the IL-6 and TNF-α production by JAWS II cells (**Figure 2B, C**, sMN1 vs. sMFN1).

The nanoparticle groups induced substantially higher IL-6 and TNF-α levels than the soluble protein mixture groups. The nanoparticle group without FliC triggered comparable cytokine production to soluble FliC, demonstrating the adjuvant efficacy of the protein nanoparticles themselves. The FliC-containing nanoparticle group produced the highest cytokines (**Figure 2B, C**, JAWS II cells, sMFN1 vs. MN1 group). In BMDCs, both MN1 and MFN1 nanoparticles induced significantly higher levels of IL-6 and TNF-α than the soluble protein mixture groups (**Figure 2B, C**, MN1 and MFN1 vs. sMFN1). These data demonstrated that nanoparticles induced higher expression of IL-6 and TNF- α by DCs.

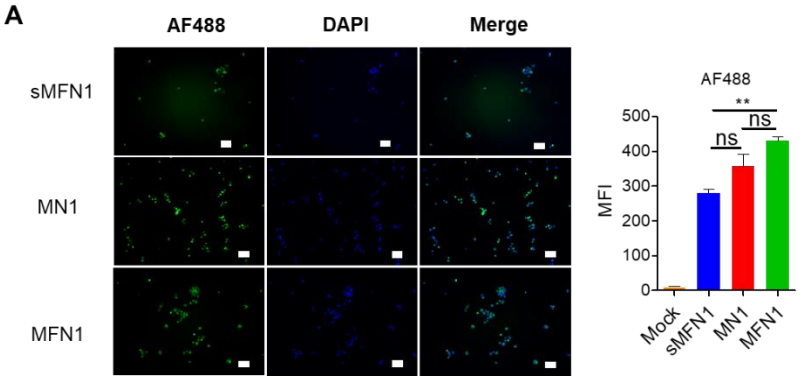

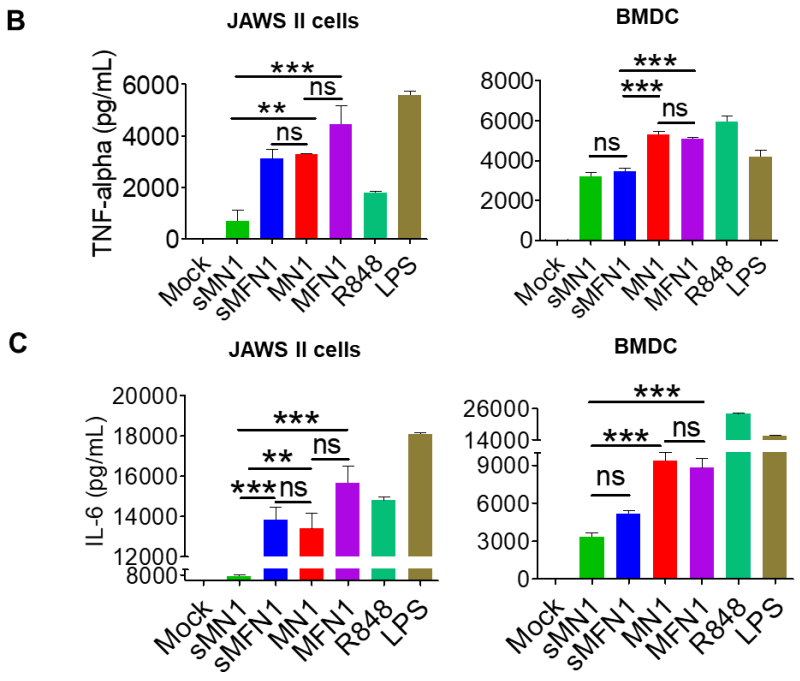

Figure 2. In-vitro internalization of MFN1 nanoparticles by dendritic cells.

A. *Fluorescence images of JAWS II cells incubated with Alexa Fluor 488-labeled soluble M2e and NA1 or MN1 or MFN1. The fluorescence intensity of AF488 was counted using mean fluorescence intensity (MFI). Bar scale, 50* μm. ***B, C.*** *Cytokines (IL-6 and TNF-α) secretion in JAWS II cells or BMDCs treated with soluble M2e and NA1 (sMN1), soluble M2e, NA1, and FliC (sMFN1), MN1, and MFN1 at a concentration of 5 μg/mL. (n = 5; **p < 0.01; ***p < 0.001; ns, p > 0.05)*

The skin vaccination strategy with MNP has been applied to improve vaccine delivery and immunogenicity. Abundant DCs and macrophages resident within the skin's dermis can be targeted by MNP administration [78]. The microneedle length in this study was 650 μm, which can fully cross the stratum corneum to deposit antigens into the viable epidermis and superficial dermal layer [79]. Dissolved MNP skin vaccination prolonged the *in vivo* kinetics of antigen release, enabling the observation of nanoparticles in the application site up to 14 days after immunization [80]. The intermediately sized nanoparticles (around 100-200nm) diffused slowly from the MNP insertion site and were transported within the more permeable regions of the extracellular matrix [81], which allowed more time for antigen-presenting cells capture. It has been

well established that prolonged antigen availability contributes to the formation of GCs, leading to enhanced antibody responses [80]. Four types of MNPs encapsulating different nanoparticles (MN1, MN2, MFN1, and MFN2) were fabricated as described previously [79]. After MNP administration to mice, Western blotting results showed that less than 30% of M2e and 20% of NA were retained in the microneedle bases (**Figure 3A**). These results indicated that MNP skin vaccination delivered 70%-80% of the MNP-loaded nanoparticles.

High-affinity antibody production is closely related to antigen persistence, B cell receptor somatic hypermutation, and B cell affinity maturation in germinal centers (GCs) [82]. CD95 and GL7 double-positive GC B cell populations were determined in ILNs on day 7 after one immunization. As shown in **Figure 3B and C,** after MFN2 MNP immunization, there were significantly increased numbers of $B220^{+}CD95^{+}GL7^{+}$ GC B cells in ILNs compared with the other groups. The MN2 MNP-immunized group also showed a higher $B220^{+}CD95^{+}GL7^{+}$ population than the sMFN2 or PBS group. Therefore, MNP skin vaccination induced enhanced germinal center reactions.

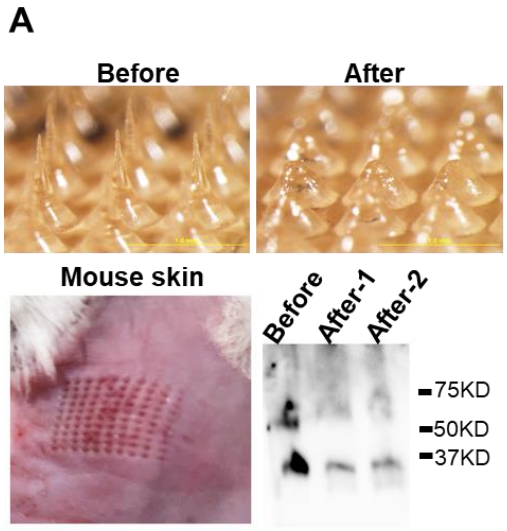

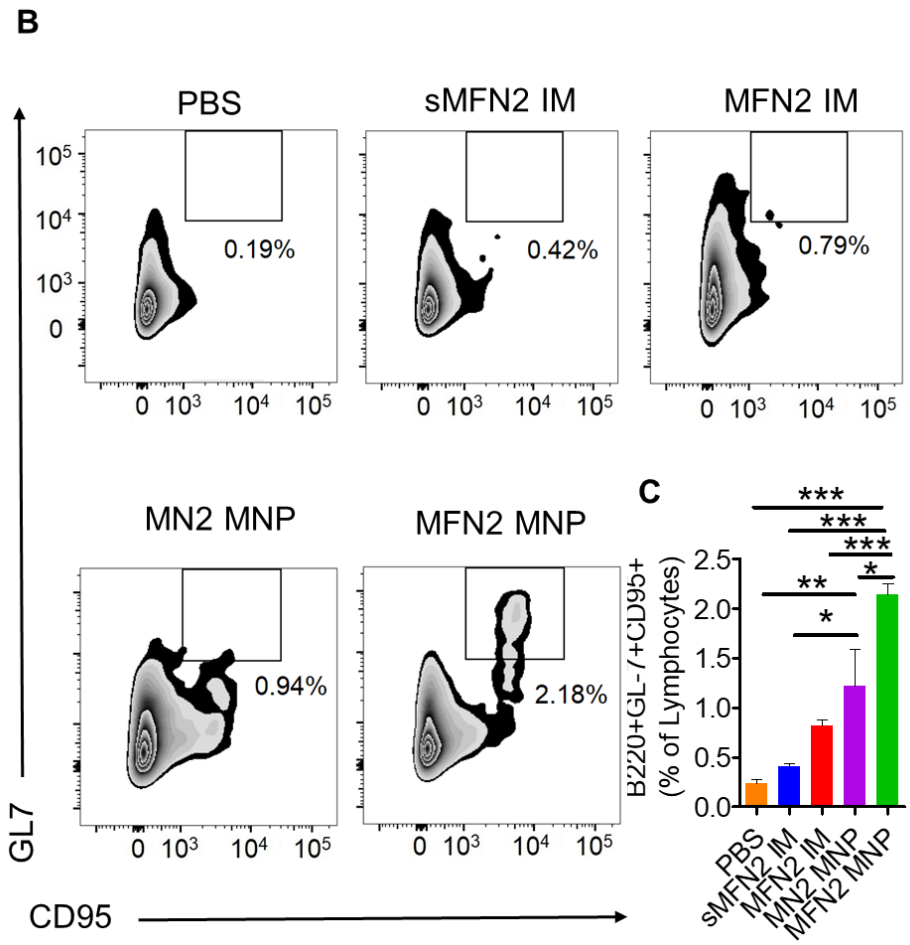

Figure 3. Vaccine-delivery* efficacies *of MNPs and germinal center immune responses
A. *A magnified view of the structure and layout of the MNP before and after attaching to the skin. Bar scale, 1.0 mm. Determination of remaining M2e-N1 nanoparticles in MNPs after sticking to the skin using anti-his antibody with the Western Blot method.* ***B, C.*** *Germinal center B cell responses in vaccinated mice. The percentage of CD95 and GL7 positive cells from inguinal lymph nodes 7 days after the primary immunization-. (n = 3; * p<0.05, **p < 0.01; ***p < 0.001; ns, p > 0.05)*

3b: Determine the immunogenicity of MFNA MNP in mice

We designed the different vaccination groups to consider IM vs. MNP delivery, soluble protein vs. nanoparticle antigens, and FliC vs. no FliC. As shown in **Figure 4A, B**, the MFN1 MNP immunization induced the highest M2e and NA1-specific antibody responses among the five

groups in the M2e-NA1 group cohort. In contrast, MN2 and MFN2 MNP immunizations induced similarly high levels of M2e and NA2-specific antibody responses in the M2e-NA2 group cohort. Neuraminidase inhibition (NAI) of immune sera correlates to NA-mediated immune protection [83]. Our NAI assay results showed that immune sera from MN1 and MN2 groups possessed potent neutralization to homologous NA influenza viruses. MFN1 and MN1 MNP and MN1 IM immune sera showed a significant decrease in OD_{450} (indicating an elevated NAI) compared with sMFN1 immune sera or untreated NA1 virus (**Figure 4C**, H5N1) up to a 20,480-fold dilution. MFN2 and MN2 MNP immune sera showed a similar inhibition, at a 20,480-fold dilution, in OD_{450} compared with untreated NA2 virus (**Figure 4C**, H3N2).

IL-4 mediates the differentiation of naïve T cells into Th2 cells and the differentiation and proliferation of B cells, driving immunoglobulin(Ig) class switching to IgG1 and memory B cell production [84, 85]. We determined the IL-4 secreting cell population at week three after boosting immunization. The MFN1 and MFN2 MNP immunizations significantly increased the numbers of M2e and NA-specific IL-4 secreting splenocytes in each group (**Figure 4D, E**).

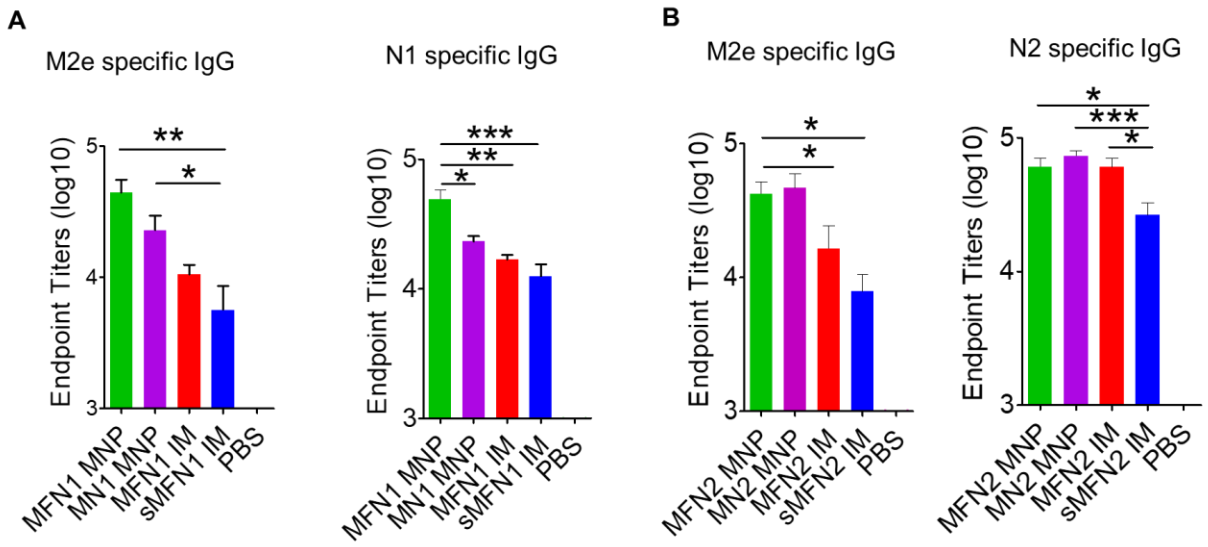

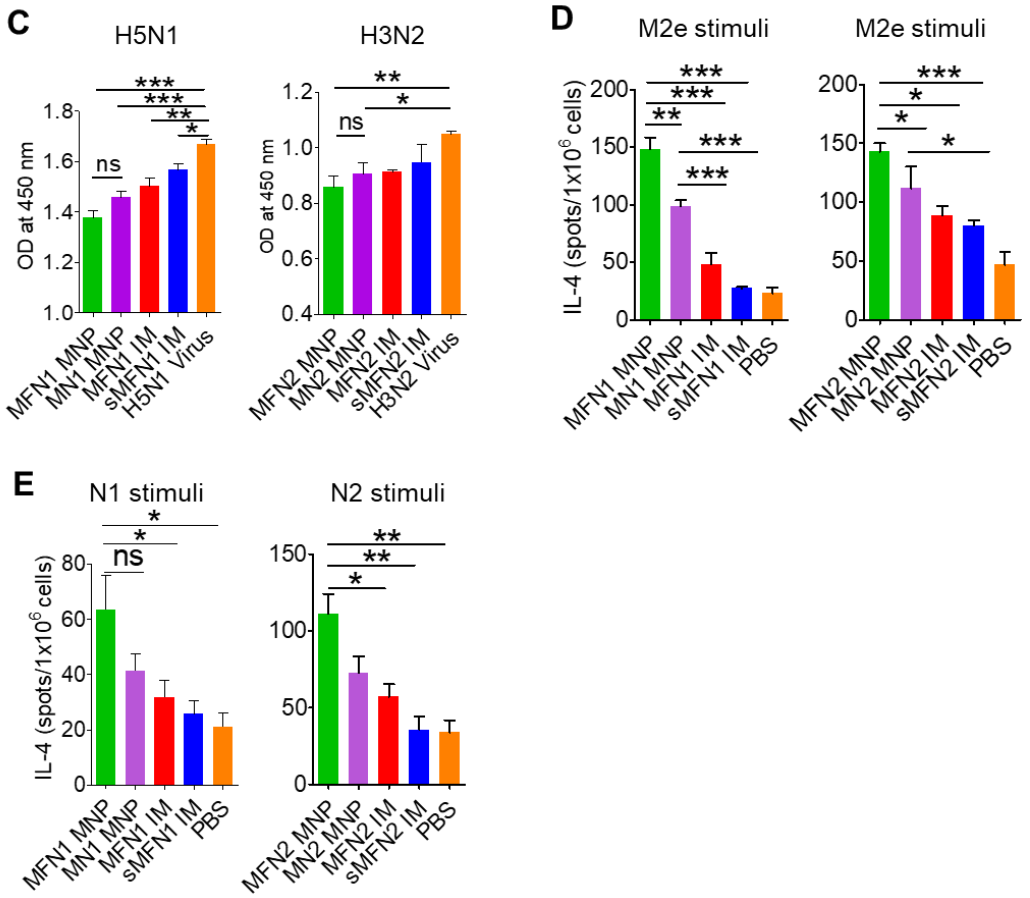

Figure 4. Humoral and cellular immune responses in vaccinated mice.
A. *M2e-specific antibody responses.* ***B.*** *NA-specific antibody responses.* ***C.*** *NA inhibition test against H5N1 or H3N2.* ***D, E.*** *Enumeration of M2e or NA activated IL-4 secreting splenocytes by ELIspot. (n = 5; * p<0.05; **p < 0.01; ***p < 0.001; ns, p > 0.05)*

3c: Determine the protective efficacy of MFNA MNP against homogeneous and heterosubtypic virus challenges

To determine immune protection against homologous viral infection, we challenged mice in the M2e-NA1 group with 5× LD_{50} reassortant A/Vietnam/1203/2004 (rViet, H5N1) and mice in the M2e-NA2 group set with 5× LD_{50} of Aichi (H3N2) (**Figure 5**). Mice receiving the MN1-MNP, MFN1-MNP, MFN1-IM or MN2-MNP, MFN2-MNP, MFN2-IM immunizations completely survived their corresponding NA virus challenges (**Figure 5A** and **C**). Mice receiving the soluble

sMFN2 immunization showed a 50% survival rate against the rViet challenge and partial protection (40% survival rate) against the homologous viral (Aichi) challenge (**Figure 5A** and **C**). To determine if the immunity protected mice against heterosubtypic NA virus, we challenged mice in the M2e-NA2 group cluster with 5× LD_{50} PR8 (H1N1) and the M2e-NA1 group cluster with 5× LD_{50} of Aichi (H3N2). Mice receiving skin MNP vaccination (MN1, MFN1, MN2, and MFN2 MNP groups) showed 100% survival. Mice receiving MFN1 or MFN2 IM vaccination resulted in an 80% survival rate to H3N2 or a 50% survival rate to the challenge of H1N1, respectively. Mice immunized with sMFN1 or sMFN2 showed a 50% survival rate to the challenge of H3N2 and H1N1, respectively (**Figure 5B** and **D**). The FliC-adjuvanted group (MFN MNP) displayed a quicker bodyweight recovery than the non-adjuvanted group (MN MNP) and an increased survival rate compared with the MFN IM group in the heterosubtypic NA influenza challenge.

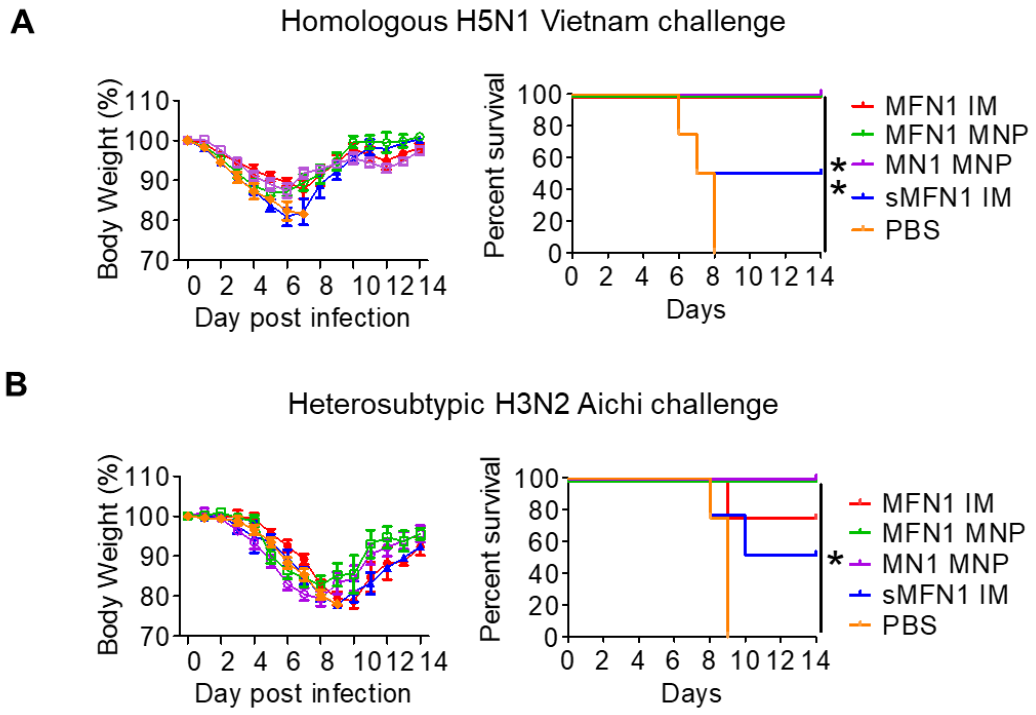

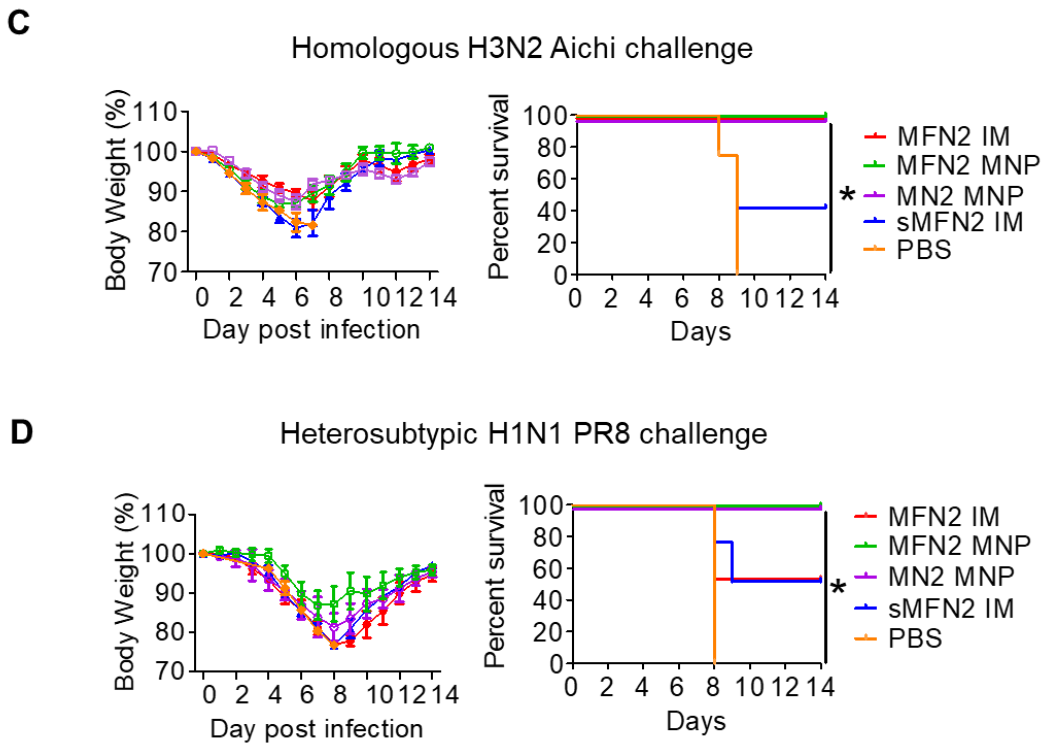

Figure 5. Immune protection against influenza viruses with homologous and heterosubtypic NA.
A, B. *Bodyweight monitoring and survival rate of NA1-Flic/M2e group set. Challenge dose:* ***A.*** *5×LD_{50} rViet (H5N1);* ***B.*** *5×LD_{50} Aichi (H3N2).* ***C, D*** *Bodyweight monitoring and survival rate of NA2-Flic/M2e group set. Challenge dose:* ***C.*** *5×LD_{50} Aichi (H3N2) challenge;* ***D.*** *5×LD_{50} PR8 (H1N1). (* $p<0.05$, ** $p < 0.01$; $n = 5$).*

Lung tissues from all the challenged mice were histologically analyzed. The MNP and IM nanoparticle groups showed less alveolar inflammation and less immune cell infiltration than the naïve infection or soluble protein mixture groups (**Figure 6A, B**). Consistent with the decreased injury scores in the layered protein nanoparticle immunized groups, all MNP skin immunization groups showed significantly reduced viral titers in the lungs than the corresponding soluble protein mixture groups (**Figure 6C**).

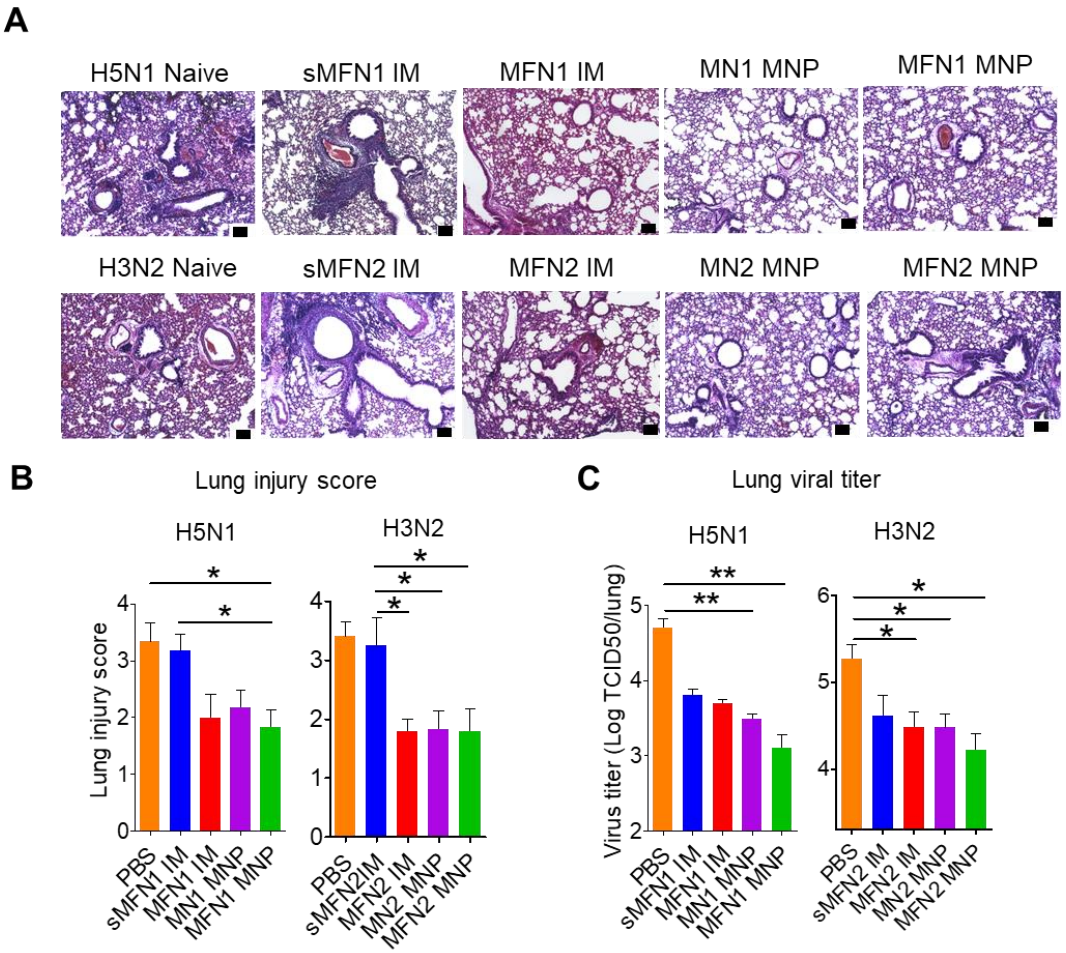

Figure 6. Histology examination and lung viral titers
A. *Histology examination by using H&E staining. Bar scale, 100* µm*.* ***B.*** *Lung injury scores of H5N1 and H3N2 infected groups.* ***C.*** *Viral titers of lungs from different immunization groups. (n = 5; * p<0.05; **p < 0.01; ***p < 0.001)*

Interferon-gamma (IFN-γ) is mainly produced by CD4 T cells and acts as a critical mediator in cellular immunity. IFN-γ is required for effector CD4 T cells to mediate lung protection and necessary for host survival [86, 87]. Antigen-specific IFN-γ-secreting CD4 T cells were analyzed after viral challenges. Compared with the MN2-MNP, MFN2-IM, and sMFN2-IM groups, MFN2-MNP immunization significantly increased the percentage of M2e and NA2-specific IFN-γ-secreting CD4 T cells in lungs five days after Aichi (H3N2) infection. However, only a moderate increase of NA2-specific IFN-γ-secreting populations was observed after MN2 MNP

immunization. The results indicate that FliC in nanoparticle MNP skin vaccination plays a vital role in inducing antigen-specific IFN-γ secretion (**Figure 7A, B**).

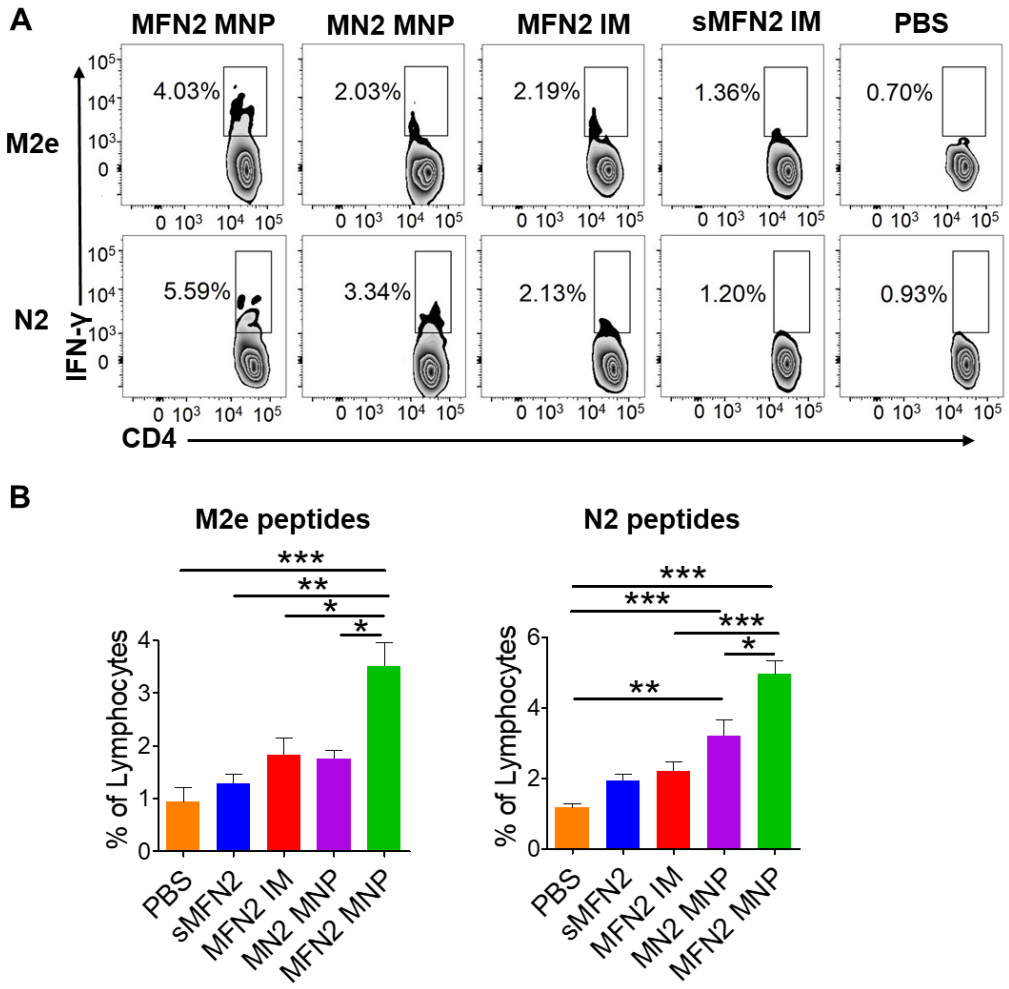

Figure 7. IFN-γ secreting CD4 T cell responses post-infection
*A. B. The percentage of IFN-γ secreting CD4 T cells from lungs of mice infected by 1× LD_{50} of H3N2. (n = 3; * p<0.05; **p < 0.01; ***p < 0.001; ns, p > 0.05)*

3.2.2 Conclusion

In summary, we have successfully fabricated layered protein nanoparticles made of relatively conserved influenza NA and M2e and a molecular adjuvant FliC. The introduction of FliC increased the antigen capture, cytokine secretion, and maturation of dendritic cells. Compared with

traditional intramuscular immunization, the MNP skin vaccination efficiently delivered antigens to skin antigen-presenting cells, inducing robust NA- and M2e-specific antibody or cellular responses. Therefore, the combination of MNP skin vaccination with MFN protein nanoparticles conferred protection against homologous and heterosubtypic NA viral infection. The self-adjuvanted MFN protein nanoparticles administered to the skin have the potential to be further developed into a standalone universal influenza vaccine or as part of a synergistic, multi-component vaccine for broad protection against influenza.

4 CONCLUSION

In summary, we have successfully fabricated layered protein nanoparticles made of relatively conserved influenza NA and M2e and a molecular adjuvant FliC. The introduction of FliC increased the antigen capture, cytokine secretion, and maturation of dendritic cells. Our results show that double-layered M2e-NA protein nanoparticles have the potential to be developed into influenza universal vaccines, either alone or as a synergistic component in more complicated influenza universal vaccine formulations. Previous studies indicated that Antibody-dependent cellular cytotoxicity (ADCC) was mediated by NA or M2e specific antibodies using Fc resceptors. Both ADCC intermediated antibody and T cell immune responses contributed to cross-protection. The incorporation of stabilized antigenic proteins into layered protein nanoparticles could be a general vaccine strategy for different pathogens. Compared with traditional intramuscular immunization, the MNP skin vaccination efficiently delivered antigens to skin antigen-presenting cells, inducing robust NA- and M2e-specific antibody or cellular responses. Therefore, universal influenza vaccines with a novel format of layered protein nanoparticles contain only antigenic proteins of interest and are highly immunogenic, inducing robust and long-lasting immunity. The nanoparticles are approximately the size of influenza virions and have a core of M2e displaying a shell of conserved influenza surface antigens. The nanoparticle fabrication avoids the risk of the instability of VLPs or other vesicle particles under osmotic stresses or changes in salt concentration and prevents off-target immune responses against self-assembly motifs found in other protein nanoparticle designs. The reducibility of the crosslinker DTSSP by intracellular thiols provides a slow release of free antigenic proteins after uptake by APCs. Meanwhile, the abiotic nature of the protein nanoparticles also enhances their amenability to a cold chain-independent storage.

Currently, several universal influenza vaccines are in their early phases of clinical trials. We can foresee some candidates can be tested for a later phase of efficacy trials in five years. Integrated with novel approaches for drug delivery and controlled release, like dissolvable microneedle patch-based skin vaccination, a convenient, syringe-free and painless, self-administrated affordable universal influenza vaccine can be available in eight to ten years.

APPENDICES

Publications

1. **Ye Wang**, Song Li, Chunhong Dong, et al. Skin vaccination with dissolvable microneedle patches incorporating influenza neuraminidase and flagellin protein nanoparticles induces broad immune protection against multiple influenza viruses. ACS Applied Biomaterials, 2021
2. Chunhong Dong, **Ye Wang**, Gilbert X. Gonzalez, et al. Intranasal Vaccination with Influenza HA/GO-PEI Nanoparticles Provides Immune Protection against Homo- and Heterologous Strains. Proc Natl Acad Sci U S A, 2021, 118 (19)
3. **Ye Wang**, Lei Deng, Gilbert X. Gonzalez, et al. Double-Layered M2e-NA Protein Nanoparticle Immunization Induces Broad Cross-Protection against Different Influenza Viruses in Mice. Adv Healthc Mater, 2020. 9(2): p. e1901176
4. Lei Deng, Timothy Chang, **Ye Wang**, et al. Heterosubtypic influenza protection elicited by double-layered polypeptide nanoparticles in mice. Proc Natl Acad Sci U S A, 2018. 115(33): p. E7758-E7767.
5. **Ye Wang**, Lei Deng, Sang-Moo Kang, et al. Universal influenza vaccines: from viruses to nanoparticles. Expert Rev Vaccines, 2018. 17(11): p. 967-976. (Review)
6. **Ye Wang**, Yu-Jing Jung, Ki-Hye Kim et al. Antiviral Activity of Fermented Ginseng Extracts against a Broad Range of Influenza Viruses. Viruses, 2018. 10(9).
7. Lei Deng, Teena Mohan, Timothy Chang, Gilbert X. Gonzalez, **Ye Wang**, et al. Double-layered protein nanoparticles induce broad protection against divergent influenza A viruses. Nat Commun 9, 359 (2018).
8. Teena Mohan, Wandi Zhu, **Ye Wang**, et al. Applications of chemokines as adjuvants for vaccine immunotherapy. Immunobiology, 2018. 223(6-7): p. 477-485. (Review)

REFERENCES

1. Chandra, S., *Deaths associated with influenza pandemic of 1918-19, Japan.* Emerg Infect Dis, 2013. **19**(4): p. 616-22.
2. Allen, P.J., *Avian influenza pandemic: not if, but when.* Pediatr Nurs, 2006. **32**(1): p. 76-81.
3. CDC, *CDC seasonal flu vaccine effectiveness studies.* 2021.
4. CDC, *Summary of the 2014-2015 Influenza Season.* 2016.
5. Flannery, B., et al., *Interim Estimates of 2017-18 Seasonal Influenza Vaccine Effectiveness - United States, February 2018.* MMWR Morb Mortal Wkly Rep, 2018. **67**(6): p. 180-185.
6. Chow, E.J., et al., *Update: Influenza Activity - United States and Worldwide, May 20-October 13, 2018.* MMWR Morb Mortal Wkly Rep, 2018. **67**(42): p. 1178-1185.
7. Mei, L., et al., *Changes in and shortcomings of control strategies, drug stockpiles, and vaccine development during outbreaks of avian influenza A H5N1, H1N1, and H7N9 among humans.* Biosci Trends, 2013. **7**(2): p. 64-76.
8. Gao, R., et al., *Human infection with a novel avian-origin influenza A (H7N9) virus.* N Engl J Med, 2013. **368**(20): p. 1888-97.
9. Sautto, G.A., G.A. Kirchenbaum, and T.M. Ross, *Towards a universal influenza vaccine: different approaches for one goal.* Virol J, 2018. **15**(1): p. 17.
10. Eliasson, D.G., et al., *M2e-tetramer-specific memory CD4 T cells are broadly protective against influenza infection.* Mucosal Immunol, 2018. **11**(1): p. 273-289.
11. Wu, N.C. and I.A. Wilson, *A Perspective on the Structural and Functional Constraints for Immune Evasion: Insights from Influenza Virus.* J Mol Biol, 2017. **429**(17): p. 2694-2709.
12. Kaminski, D.A. and F.E. Lee, *Antibodies against conserved antigens provide opportunities for reform in influenza vaccine design.* Front Immunol, 2011. **2**: p. 76.
13. McAuley, J.L., et al., *Influenza Virus Neuraminidase Structure and Functions.* Front Microbiol, 2019. **10**: p. 39.
14. Vavricka, C.J., et al., *Influenza neuraminidase operates via a nucleophilic mechanism and can be targeted by covalent inhibitors.* Nat Commun, 2013. **4**: p. 1491.
15. Johansson, B.E. and E.D. Kilbourne, *Immunization with purified N1 and N2 influenza virus neuraminidases demonstrates cross-reactivity without antigenic competition.* Proc Natl Acad Sci U S A, 1994. **91**(6): p. 2358-61.
16. Westgeest, K.B., et al., *Genomewide analysis of reassortment and evolution of human influenza A(H3N2) viruses circulating between 1968 and 2011.* J Virol, 2014. **88**(5): p. 2844-57.
17. Doyle, T.M., et al., *Universal anti-neuraminidase antibody inhibiting all influenza A subtypes.* Antiviral Res, 2013. **100**(2): p. 567-74.
18. Chen, Y.Q., et al., *Influenza Infection in Humans Induces Broadly Cross-Reactive and Protective Neuraminidase-Reactive Antibodies.* Cell, 2018. **173**(2): p. 417-429 e10.
19. Wan, H., et al., *Structural characterization of a protective epitope spanning A(H1N1)pdm09 influenza virus neuraminidase monomers.* Nat Commun, 2015. **6**: p. 6114.
20. Krammer, F., et al., *NAction! How Can Neuraminidase-Based Immunity Contribute to Better Influenza Virus Vaccines?* mBio, 2018. **9**(2).

21. Gao, R., et al., *Influenza A Virus Antibodies with Antibody-Dependent Cellular Cytotoxicity Function.* Viruses, 2020. **12**(3).
22. He, W., et al., *Broadly neutralizing anti-influenza virus antibodies: enhancement of neutralizing potency in polyclonal mixtures and IgA backbones.* J Virol, 2015. **89**(7): p. 3610-8.
23. Stadlbauer, D., et al., *Broadly protective human antibodies that target the active site of influenza virus neuraminidase.* Science, 2019. **366**(6464): p. 499-504.
24. Samji, T., *Influenza A: understanding the viral life cycle.* Yale J Biol Med, 2009. **82**(4): p. 153-9.
25. Liu, W., et al., *Sequence comparison between the extracellular domain of M2 protein human and avian influenza A virus provides new information for bivalent influenza vaccine design.* Microbes Infect, 2005. **7**(2): p. 171-7.
26. Kang, S.M., M.C. Kim, and R.W. Compans, *Virus-like particles as universal influenza vaccines.* Expert Rev Vaccines, 2012. **11**(8): p. 995-1007.
27. Wang, B.Z., et al., *Enhanced influenza virus-like particle vaccines containing the extracellular domain of matrix protein 2 and a Toll-like receptor ligand.* Clin Vaccine Immunol, 2012. **19**(8): p. 1119-25.
28. Kim, M.C., et al., *Virus-like particles containing multiple M2 extracellular domains confer improved cross-protection against various subtypes of influenza virus.* Mol Ther, 2013. **21**(2): p. 485-92.
29. Karch, C.P., et al., *Vaccination with self-adjuvanted protein nanoparticles provides protection against lethal influenza challenge.* Nanomedicine, 2017. **13**(1): p. 241-251.
30. Qi, M., et al., *Intranasal Nanovaccine Confers Homo- and Hetero-Subtypic Influenza Protection.* Small, 2018. **14**(13): p. e1703207.
31. Weinberger, B., *Vaccines for the elderly: current use and future challenges.* Immun Ageing, 2018. **15**: p. 3.
32. Smith, L.E., et al., *A systematic review of factors affecting vaccine uptake in young children.* Vaccine, 2017. **35**(45): p. 6059-6069.
33. Zhu, F.C., et al., *A novel influenza A (H1N1) vaccine in various age groups.* N Engl J Med, 2009. **361**(25): p. 2414-23.
34. Miller, J.R., H.A. Orgel, and E.O. Meltzer, *The safety of egg-containing vaccines for egg-allergic patients.* J Allergy Clin Immunol, 1983. **71**(6): p. 568-73.
35. Pugliese, R. and F. Gelain, *Peptidic Biomaterials: From Self-Assembling to Regenerative Medicine.* Trends Biotechnol, 2017. **35**(2): p. 145-158.
36. Padilla, J.E., C. Colovos, and T.O. Yeates, *Nanohedra: using symmetry to design self assembling protein cages, layers, crystals, and filaments.* Proc Natl Acad Sci U S A, 2001. **98**(5): p. 2217-21.
37. Ardejani, M.S. and B.P. Orner, *Materials science. Obey the peptide assembly rules.* Science, 2013. **340**(6132): p. 561-2.
38. Deng, L., et al., *Protein nanoparticle vaccine based on flagellin carrier fused to influenza conserved epitopes confers full protection against influenza A virus challenge.* Virology, 2017. **509**: p. 82-89.
39. Yassine, H.M., et al., *Hemagglutinin-stem nanoparticles generate heterosubtypic influenza protection.* Nat Med, 2015. **21**(9): p. 1065-70.
40. Verma, D., et al., *Protein Based Nanostructures for Drug Delivery.* J Pharm (Cairo), 2018. **2018**: p. 9285854.

41. Ashok, A., M. Brison, and Y. LeTallec, *Improving cold chain systems: Challenges and solutions.* Vaccine, 2017. **35**(17): p. 2217-2223.
42. Chang, T.Z., et al., *H7 Hemagglutinin nanoparticles retain immunogenicity after >3 months of 25 degrees C storage.* PLoS One, 2018. **13**(8): p. e0202300.
43. Mizel, S.B. and J.T. Bates, *Flagellin as an adjuvant: cellular mechanisms and potential.* J Immunol, 2010. **185**(10): p. 5677-82.
44. Wang, B.Z., et al., *Intranasal immunization with influenza VLPs incorporating membrane-anchored flagellin induces strong heterosubtypic protection.* PLoS One, 2010. **5**(11): p. e13972.
45. Wang, B.Z., et al., *Incorporation of membrane-anchored flagellin into influenza virus-like particles enhances the breadth of immune responses.* J Virol, 2008. **82**(23): p. 11813-23.
46. Hayashi, F., et al., *The innate immune response to bacterial flagellin is mediated by Toll-like receptor 5.* Nature, 2001. **410**(6832): p. 1099-103.
47. Turley, C.B., et al., *Safety and immunogenicity of a recombinant M2e-flagellin influenza vaccine (STF2.4xM2e) in healthy adults.* Vaccine, 2011. **29**(32): p. 5145-52.
48. Vassilieva, E.V., et al., *Enhanced mucosal immune responses to HIV virus-like particles containing a membrane-anchored adjuvant.* mBio, 2011. **2**(1): p. e00328-10.
49. Heath, W.R. and F.R. Carbone, *The skin-resident and migratory immune system in steady state and memory: innate lymphocytes, dendritic cells and T cells.* Nat Immunol, 2013. **14**(10): p. 978-85.
50. Chandrasekhar, S., et al., *Microarrays and microneedle arrays for delivery of peptides, proteins, vaccines and other applications.* Expert Opin Drug Deliv, 2013. **10**(8): p. 1155-70.
51. Zaric, M., et al., *Dissolving microneedle delivery of nanoparticle-encapsulated antigen elicits efficient cross-priming and Th1 immune responses by murine Langerhans cells.* J Invest Dermatol, 2015. **135**(2): p. 425-434.
52. Gill, H.S., et al., *Effect of microneedle design on pain in human volunteers.* Clin J Pain, 2008. **24**(7): p. 585-94.
53. Birchall, J.C., et al., *Microneedles in clinical practice--an exploratory study into the opinions of healthcare professionals and the public.* Pharm Res, 2011. **28**(1): p. 95-106.
54. Quan, F.S., et al., *Intradermal vaccination with influenza virus-like particles by using microneedles induces protection superior to that with intramuscular immunization.* J Virol, 2010. **84**(15): p. 7760-9.
55. Quan, F.S., et al., *Long-term protective immunity from an influenza virus-like particle vaccine administered with a microneedle patch.* Clin Vaccine Immunol, 2013. **20**(9): p. 1433-9.
56. Kim, M.C., et al., *Microneedle patch delivery to the skin of virus-like particles containing heterologous M2e extracellular domains of influenza virus induces broad heterosubtypic cross-protection.* J Control Release, 2015. **210**: p. 208-16.
57. Deng, L., et al., *Heterosubtypic influenza protection elicited by double-layered polypeptide nanoparticles in mice.* Proc Natl Acad Sci U S A, 2018.
58. Deng, L., et al., *Double-layered protein nanoparticles induce broad protection against divergent influenza A viruses.* Nat Commun, 2018. **9**(1): p. 359.
59. Russell, R.J., et al., *The structure of H5N1 avian influenza neuraminidase suggests new opportunities for drug design.* Nature, 2006. **443**(7107): p. 45-9.

60. Stetefeld, J., et al., *Crystal structure of a naturally occurring parallel right-handed coiled coil tetramer.* Nat Struct Biol, 2000. **7**(9): p. 772-6.
61. Schmidt, P.M., et al., *A generic system for the expression and purification of soluble and stable influenza neuraminidase.* PLoS One, 2011. **6**(2): p. e16284.
62. Boehm, U., et al., *Cellular responses to interferon-gamma.* Annu Rev Immunol, 1997. **15**: p. 749-95.
63. Paul, W.E., *Interleukin 4: signalling mechanisms and control of T cell differentiation.* Ciba Found Symp, 1997. **204**: p. 208-16; discussion 216-9.
64. Pedersen, J.C., *Neuraminidase-inhibition assay for the identification of influenza A virus neuraminidase subtype or neuraminidase antibody specificity.* Methods Mol Biol, 2008. **436**: p. 67-75.
65. Wohlbold, T.J., et al., *Vaccination with adjuvanted recombinant neuraminidase induces broad heterologous, but not heterosubtypic, cross-protection against influenza virus infection in mice.* mBio, 2015. **6**(2): p. e02556.
66. Deng, L., et al., *Heterosubtypic influenza protection elicited by double-layered polypeptide nanoparticles in mice.* Proc Natl Acad Sci U S A, 2018. **115**(33): p. E7758-E7767.
67. Assarsson, E., et al., *Immunomic analysis of the repertoire of T-cell specificities for influenza A virus in humans.* J Virol, 2008. **82**(24): p. 12241-51.
68. Roman, E., et al., *CD4 effector T cell subsets in the response to influenza: heterogeneity, migration, and function.* J Exp Med, 2002. **196**(7): p. 957-68.
69. Flynn, K.J., et al., *Virus-specific CD8+ T cells in primary and secondary influenza pneumonia.* Immunity, 1998. **8**(6): p. 683-91.
70. McElhaney, J.E., et al., *The immune response to influenza in older humans: beyond immune senescence.* Immun Ageing, 2020. **17**: p. 10.
71. Wang, Y., et al., *Double-Layered M2e-NA Protein Nanoparticle Immunization Induces Broad Cross-Protection against Different Influenza Viruses in Mice.* Adv Healthc Mater, 2020. **9**(2): p. e1901176.
72. Lambert, W., et al., *Thiol-exchange in DTSSP crosslinked peptides is proportional to cysteine content and precisely controlled in crosslink detection by two-step LC-MALDI MSMS.* Protein Sci, 2011. **20**(10): p. 1682-91.
73. Wang, C., W. Zhu, and B.Z. Wang, *Dual-linker gold nanoparticles as adjuvanting carriers for multivalent display of recombinant influenza hemagglutinin trimers and flagellin improve the immunological responses in vivo and in vitro.* Int J Nanomedicine, 2017. **12**: p. 4747-4762.
74. Gill, H.S., et al., *Cutaneous immunization: an evolving paradigm in influenza vaccines.* Expert Opin Drug Deliv, 2014. **11**(4): p. 615-27.
75. Rodgers, A.M., A.S. Cordeiro, and R.F. Donnelly, *Technology update: dissolvable microneedle patches for vaccine delivery.* Med Devices (Auckl), 2019. **12**: p. 379-398.
76. Verboogen, D.R.J., et al., *Interleukin-6 secretion is limited by self-signaling in endosomes.* J Mol Cell Biol, 2019. **11**(2): p. 144-157.
77. Blanco, P., et al., *Dendritic cells and cytokines in human inflammatory and autoimmune diseases.* Cytokine Growth Factor Rev, 2008. **19**(1): p. 41-52.
78. Malissen, B., S. Tamoutounour, and S. Henri, *The origins and functions of dendritic cells and macrophages in the skin.* Nat Rev Immunol, 2014. **14**(6): p. 417-28.

79. Zhu, W., et al., *A boosting skin vaccination with dissolving microneedle patch encapsulating M2e vaccine broadens the protective efficacy of conventional influenza vaccines.* J Control Release, 2017. **261**: p. 1-9.
80. Boopathy, A.V., et al., *Enhancing humoral immunity via sustained-release implantable microneedle patch vaccination.* Proc Natl Acad Sci U S A, 2019. **116**(33): p. 16473-16478.
81. Irvine, D.J., M.A. Swartz, and G.L. Szeto, *Engineering synthetic vaccines using cues from natural immunity.* Nat Mater, 2013. **12**(11): p. 978-90.
82. Stebegg, M., et al., *Regulation of the Germinal Center Response.* Front Immunol, 2018. **9**: p. 2469.
83. Monto, A.S., et al., *Antibody to Influenza Virus Neuraminidase: An Independent Correlate of Protection.* J Infect Dis, 2015. **212**(8): p. 1191-9.
84. Chen, L., et al., *IL-4 induces differentiation and expansion of Th2 cytokine-producing eosinophils.* J Immunol, 2004. **172**(4): p. 2059-66.
85. Saito, T., et al., *Effective collaboration between IL-4 and IL-21 on B cell activation.* Immunobiology, 2008. **213**(7): p. 545-55.
86. Doherty, P.C., et al., *Effector CD4+ and CD8+ T-cell mechanisms in the control of respiratory virus infections.* Immunol Rev, 1997. **159**: p. 105-17.
87. Brown, D.M., et al., *Multifunctional CD4 cells expressing gamma interferon and perforin mediate protection against lethal influenza virus infection.* J Virol, 2012. **86**(12): p. 6792-803.